

1 **Mitochondrial respiratory states and rates:**  
2 **Building blocks of mitochondrial physiology**  
3 **Part 1.** MitoEAGLE preprint 2018-02-26(30)

4  
5 [http://www.mitoeagle.org/index.php/MitoEAGLE\\_preprint\\_2018-02-08](http://www.mitoeagle.org/index.php/MitoEAGLE_preprint_2018-02-08)

6 Preprint version 30 (2018-02-26)

7  
8 **MitoEAGLE Network**

9 Corresponding author: Gnaiger E

10 Contributing co-authors

11 Aasander Frostner E, Acuna-Castroviejo D, Ahn B, Alves MG, Amati F, Aral C,  
12 Arandarčikaitė O, Bailey DM, Bakker BM, Bastos Sant'Anna Silva AC, Battino M, Beard  
13 DA, Ben-Shachar D, Bishop D, Borutaitė V, Breton S, Brown GC, Brown RA, Buettner GR,  
14 Burtscher J, Calabria E, Calbet JA, Cardoso LHD, Carvalho E, Casado Pinna M, Cervinkova  
15 Z, Chang SC, Chaurasia B, Chen Q, Chicco AJ, Chinopoulos C, Clementi E, Coen PM, Collin  
16 A, Crisóstomo L, Das AM, Davis MS, De Palma C, Dias TR, Distefano G, Doerrier C,  
17 Drahotka Z, Duchon MR, Ehinger J, Elmer E, Endlicher R, Fell DA, Ferko M, Ferreira JCB,  
18 Filipovska A, Fisar Z, Fischer M, Fisher JJ, Fornaro M, Galkin A, Garcia-Roves PM, Garcia-  
19 Souza LF, Genova ML, Giovarelli M, Gonzalez-Armenta JL, Gonzalo H, Goodpaster BH,  
20 Gorr TA, Gourlay CW, Granata C, Grefte S, Haas CB, Haavik J, Han J, Harrison DK,  
21 Hellgren KT, Hernansanz-Agustin P, Holland O, Hoppel CL, Houstek J, Hunger M, Iglesias-  
22 Gonzalez J, Irving BA, Iyer S, Jackson CB, Jadiya P, Jang DH, Jansen-Dürr P, Jespersen NR,  
23 Jha RK, Kaambre T, Kane DA, Kappler L, Karabatsiakos A, Keijer J, Keppner G,  
24 Klingenspor M, Komlodi T, Koopman WJH, Kopitar-Jerala N, Krako Jakovljevic N, Kuang J,  
25 Kucera O, Labieniec-Watala M, Lai N, Laner V, Larsen TS, Lee HK, Leeuwenburgh C,  
26 Lemieux H, Lerfall J, Liu J, Lucchinetti E, MacMillan-Crow LA, Makrečka-Kuka M, Malik  
27 A, Markova M, Meszaros AT, Michalak S, Moiso N, Molina AJA, Montaigne D, Moore AL,  
28 Moreira BP, Mracek T, Muntane J, Muntean DM, Murray AJ, Nemeč M, Neuzil J, Newsom  
29 S, Nozickova K, O'Gorman D, Oliveira MT, Oliveira PF, Oliveira PJ, Orynbayeva Z, Pak  
30 YK, Palmeira CM, Patel HH, Pecina P, Pelena D, Pereira da Silva Grilo da Silva F, Pesta D,  
31 Petit PX, Pichaud N, Piel S, Pirkmajer S, Porter RK, Pranger F, Prochownik EV,  
32 Pulinilkunnil T, Puurand M, Radenkovic F, Radi R, Ramzan R, Reboredo P, Renner-Sattler  
33 K, Robinson MM, Rohlena J, Ropelle ER, Røslund GV, Rossiter HB, Rybacka-Mossakowska  
34 J, Saada A, Safaei Z, Salvadego D, Sandi C, Scatena R, Schartner M, Scheibye-Knudsen M,  
35 Schilling JM, Schlattner U, Schönfeld P, Schwarzer C, Scott GR, Shabalina IG, Sharma P,  
36 Sharma V, Shevchuk I, Siewiera K, Silber AM, Singer D, Smenes BT, Soares FAA, Sobotka  
37 O, Sokolova I, Spinazzi M, Stankova P, Stier A, Stocker R, Sumbalova Z, Suravajhala P,  
38 Swerdlow RH, Swiniuch D, Tanaka M, Tandler B, Tepp K, Tomar D, Towheed A, Tretter L,  
39 Trifunovic A, Trivigno C, Tronstad KJ, Trougakos IP, Tyrrell DJ, Urban T, Valentine JM,  
40 Velika B, Vendelin M, Vercesi AE, Victor VM, Villena JA, Vitorino RMP, Vogt S, Volani C,  
41 Votion DM, Vujacic-Mirski K, Wagner BA, Ward ML, Watala C, Wei YH, Wieckowski MR,  
42 Williams C, Wohlgend M, Wolff J, Wuest RCI, Zaugg K, Zaugg M, Zischka H, Zorzano A

43  
44 Supporting co-authors:

45 Bernardi P, Boetker HE, Borsheim E, Bouitbir J, Calzia E, Coker RH, Dubouchaud H,  
46 Durham WJ, Dyrstad SE, Engin AB, Gan Z, Garlid KD, Garten A, Haendeler J, Hand SC,  
47 Hepple RT, Hickey AJ, Hoel F, Kainulainen H, Khamoui AV, Kowaltowski AJ, Krajcova A,  
48 Lane N, Lenaz G, Liu SS, Mazat JP, Menze MA, Methner A, Nedergaard J, Pallotta ML,  
49 Parajuli N, Pettersen IK, Porter C, Salin K, Sazanov LA, Skolik R, Sonkar VK, Szabo I,  
50 Tavernarakis N, Thyfault JP, Vieyra A

51

**Updates and discussion:**

[http://www.mitoeagle.org/index.php/MitoEAGLE\\_preprint\\_2018-02-08](http://www.mitoeagle.org/index.php/MitoEAGLE_preprint_2018-02-08)

Correspondence: Gnaiger E

*Chair COST Action CA15203 MitoEAGLE* – <http://www.mitoeagle.org>

*Department of Visceral, Transplant and Thoracic Surgery, D. Swarovski Research  
Laboratory, Medical University of Innsbruck, Innrain 66/4, A-6020 Innsbruck, Austria*

*Email: mitoeagle@i-med.ac.at*

*Tel: +43 512 566796, Fax: +43 512 566796 20*

**Contents****Abstract****Executive summary****1. Introduction** – Box 1: In brief: Mitochondria and Bioblasts**2. Oxidative phosphorylation and coupling states in mitochondrial preparations**

Mitochondrial preparations

*2.1. Respiratory control and coupling*

The steady-state

Specification of biochemical dose

Phosphorylation,  $P_{\gg}$ , and  $P_{\gg}/O_2$  ratio

Control and regulation

Respiratory control and response

Respiratory coupling control and ET-pathway control

Coupling

Uncoupling

*2.2. Coupling states and respiratory rates*

Respiratory capacities in coupling control states

LEAK, OXPHOS, ET, ROX

Quantitative relations

*2.3. Classical terminology for isolated mitochondria*

States 1–5

**3. Normalization: fluxes and flows***3.1. Normalization: system or sample*

Flow per system,  $I$

Extensive quantities

Size-specific quantities – Box 2: Metabolic fluxes and flows: vectorial and scalar

*3.2. Normalization for system-size: flux per chamber volume*

System-specific flux,  $J_{V,O_2}$

*3.3. Normalization: per sample*

Sample concentration,  $C_{mX}$

Mass-specific flux,  $J_{O_2/mX}$

Number concentration,  $C_{NX}$

Flow per object,  $I_{O_2/X}$

*3.4. Normalization for mitochondrial content*

Mitochondrial concentration,  $C_{mtE}$ , and mitochondrial markers

Mitochondria-specific flux,  $J_{O_2/mtE}$

*3.5. Evaluation of mitochondrial markers**3.6. Conversion: units***4. Conclusions** – Box 3: Mitochondrial and cell respiration**5. References**

103 **Abstract** As the knowledge base and importance of mitochondrial physiology to human health  
104 expands, the necessity for harmonizing nomenclature concerning mitochondrial respiratory  
105 states and rates has become increasingly apparent. Clarity of concept and consistency of  
106 nomenclature are key trademarks of a research field. These trademarks facilitate effective  
107 transdisciplinary communication, education, and ultimately further discovery. The  
108 chemiosmotic theory establishes the mechanism of energy transformation and coupling in  
109 oxidative phosphorylation. The unifying concept of the protonmotive force provides the  
110 framework for developing a consistent theoretical foundation of mitochondrial physiology and  
111 bioenergetics. We follow IUPAC guidelines on terminology in physical chemistry, extended  
112 by considerations on open systems and irreversible thermodynamics. The concept-driven  
113 constructive terminology incorporates the meaning of each quantity and aligns concepts and  
114 symbols to the nomenclature of classical bioenergetics. In the frame of COST Action  
115 MitoEAGLE open to global bottom-up input, we endeavour to provide a balanced view on  
116 mitochondrial respiratory control and a critical discussion on reporting data of mitochondrial  
117 respiration in terms of metabolic flows and fluxes. Uniform standards for evaluation of  
118 respiratory states and rates will ultimately support the development of databases of  
119 mitochondrial respiratory function in species, tissues, and cells.

120

121 *Keywords:* Mitochondrial respiratory control, coupling control, mitochondrial  
122 preparations, protonmotive force, uncoupling, oxidative phosphorylation, OXPHOS,  
123 efficiency, electron transfer, ET; proton leak, LEAK, residual oxygen consumption, ROX, State  
124 2, State 3, State 4, normalization, flow, flux, O<sub>2</sub>

125

126

127

---

## 128 **Executive summary**

129

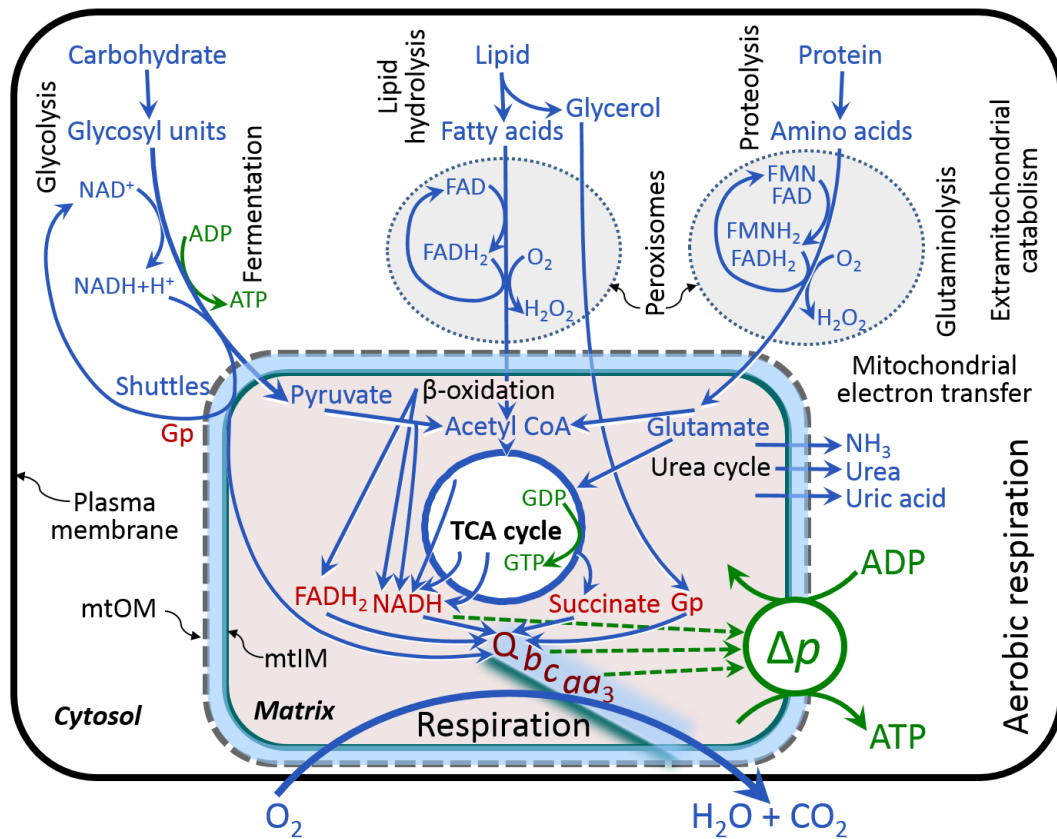
130 1. In view of broad implications on health care, mitochondrial researchers face an  
131 increasing responsibility to disseminate their fundamental knowledge and novel  
132 discoveries to a wide range of stakeholders and scientists beyond the group of  
133 specialists. This requires implementation of a commonly accepted terminology  
134 within the discipline and standardization in the translational context. Authors,  
135 reviewers, journal editors, and lecturers are challenged to collaborate with the aim  
136 to harmonize the nomenclature in the growing field of mitochondrial physiology  
137 and bioenergetics.

138 2. Aerobic energy metabolism in mitochondria of most eukaryotic cells depends on the  
139 coupling of phosphorylation ( $\text{ADP} \rightarrow \text{ATP}$ ) to O<sub>2</sub> flux in catabolic reactions. In this  
140 process of oxidative phosphorylation, coupling is mediated by translocation of  
141 protons through respiratory proton pumps operating across the inner mitochondrial  
142 membrane and generating or utilizing the protonmotive force measured between  
143 the mitochondrial matrix and intermembrane compartment. Compartmental  
144 coupling thus distinguishes vectorial oxidative phosphorylation from fermentation  
145 as the counterpart of cellular core energy metabolism (**Fig. 1**).

146 3. To exclude fermentation and other cytosolic interactions from exerting an effect on  
147 mitochondrial metabolism, the barrier function of the plasma membrane must be  
148 disrupted. Selective removal or permeabilization of the plasma membrane yields  
149 mitochondrial preparations—including isolated mitochondria, tissue and cellular  
150 preparations—with structural and functional integrity. Then extra-mitochondrial  
151 concentrations of fuel substrates transported into the mitochondrial matrix, ADP,  
152 ATP, inorganic phosphate, and cations including H<sup>+</sup> can be controlled to determine  
153 mitochondrial function under a set of conditions defined as coupling control states.

154  
155  
156  
157

A concept-driven terminology of bioenergetics incorporates in its terms and symbols explicit information on the nature of respiratory states, that makes the technical terms readily recognized and easy to understand.



158  
159  
160  
161  
162  
163  
164  
165  
166  
167  
168  
169  
170  
171  
172  
173  
174  
175  
176  
177  
178  
179  
180  
181  
182

**Fig. 1. Respiration in the framework of cellular catabolic energy metabolism.** Aerobic respiration is the utilization of the products of extra-mitochondrial catabolism as fuel substrates for electron transfer to  $O_2$  as the electron acceptor. In core pathways of energy metabolism, catabolic reactions are coupled to the phosphorylation of ADP to ATP, with energy transformation mediated by the protonmotive force,  $\Delta p$ . Anabolic reactions are tightly integrated with catabolism, both by ATP as the intermediary energy currency and by small organic precursor molecules as building blocks for biosynthesis (not shown). Glycolysis involves substrate-level phosphorylation of ADP to ATP in anaerobic fermentation. In contrast, partial extra-mitochondrial oxidation of fatty acids and amino acids proceeds in peroxisomes without coupling to ATP production: acyl-CoA oxidase catalyzes the oxidation of FADH<sub>2</sub> with electron transfer to  $O_2$ ; amino acid oxidases oxidize FMNH<sub>2</sub> or FADH<sub>2</sub>. Mitochondrial outer and inner membrane, mtOM and mtIM. Coenzyme Q, Q, and the cytochromes *b*, *c*, and *aa*<sub>3</sub> are redox systems of the mtIM. Dashed arrows indicate the connection between the proton pumps (respiratory Complexes CI, CIII and CIV) and the transmembrane  $\Delta p$ . Glycerol-3-phosphate, Gp; tricarboxylic acid cycle, TCA cycle. Mitochondria and peroxisomes are maintained intact and associated in various mitochondrial preparations used in respiratory studies, whereas the cytosolic components are separated from the mitochondria for the analysis of oxidative phosphorylation.

4. Mitochondrial coupling states are defined according to the control of respiratory oxygen flux by the protonmotive force. Capacities of oxidative phosphorylation and electron transfer are measured at kinetically saturating concentrations of fuel substrates, ADP and inorganic phosphate, or at optimal uncoupler concentrations, respectively. Respiratory capacities are a measure of the upper bound of the rates

- 183 of respiration, providing reference values for the diagnosis of health and disease,  
184 and for evaluation of the effects of Evolutionary background, Age, Gender and sex,  
185 Lifestyle and Environment (EAGLE).
- 186 5. Some degree of uncoupling is a characteristic of energy-transformations across  
187 membranes. Uncoupling is caused by a variety of physiological, pathological,  
188 toxicological, pharmacological and environmental conditions that exert an  
189 influence not only on the proton leak and cation cycling, but also on proton slip  
190 within the proton pumps and the structural integrity of the mitochondria. A more  
191 loosely coupled state is induced by stimulation of mitochondrial superoxide  
192 formation and the bypass of proton pumps. In addition, uncoupling by application  
193 of protonophores represents an experimental intervention for the transition from a  
194 well-coupled to the noncoupled state of mitochondrial respiration.
- 195 6. Respiratory oxygen consumption rates have to be carefully normalized to enable meta-  
196 analytic studies beyond the specific question of a particular experiment. Therefore,  
197 all raw data should be published in a supplemental table or open access data  
198 repository. Normalization of rates for the volume of the experimental chamber (the  
199 measuring system) is distinguished from normalization for (1) the volume or mass  
200 of the experimental sample, (2) the number of objects (cells, organisms), and (3)  
201 the concentration of mitochondrial markers in the chamber.
- 202 7. The consistent use of terms and symbols discussed in this MitoEAGLE position  
203 statement will facilitate transdisciplinary communication and support further  
204 development of a database on bioenergetics and mitochondrial physiology. The  
205 present considerations are focused on studies with mitochondrial preparations.  
206 These will be extended in a series of reports on pathway control of mitochondrial  
207 respiration, the protonmotive force, respiratory states in intact cells, and  
208 harmonization of experimental procedures.
- 
- 209  
210  
211

---

### 212 **Box 1: In brief – Mitochondria and Bioblasts**

213 **Mitochondria** are the oxygen-consuming electrochemical generators evolved from  
214 endosymbiotic bacteria (Margulis 1970; Lane 2005). They were described by Richard Altmann  
215 (1894) as ‘bioblasts’, which include not only the mitochondria as presently defined, but also  
216 symbiotic and free-living bacteria. The word ‘mitochondria’ (Greek mitos: thread; chondros:  
217 granule) was introduced by Carl Benda (1898).

218 Mitochondria are dynamic networks contained within eukaryotic cells morphologically  
219 characterized by a double membrane. The mitochondrial inner membrane (mtIM) shows  
220 dynamic tubular to disk-shaped cristae that separate the mitochondrial matrix, *i.e.*, the  
221 negatively charged internal mitochondrial compartment, from the intermembrane space; the  
222 latter being positively charged and enclosed by the mitochondrial outer membrane (mtOM).  
223 The mtIM contains the non-bilayer phospholipid cardiolipin, which is not present in any other  
224 eukaryotic cellular membrane. Cardiolipin promotes the formation of respiratory  
225 supercomplexes (SC I<sub>n</sub>III<sub>n</sub>IV<sub>n</sub>), which are supramolecular assemblies based upon specific,  
226 though dynamic interactions between individual respiratory complexes (Greggio *et al.* 2017;  
227 Lenaz *et al.* 2017). Membrane fluidity exerts an influence on functional properties of proteins  
228 incorporated in the membranes (Waczulikova *et al.* 2007). In addition to mitochondrial  
229 movement along microtubules, mitochondrial morphology can change in response to energy  
230 requirements of the cell via processes known as fusion and fission, through which mitochondria  
231  
232



233 communicate within a network, and in response to intracellular stress factors causing swelling  
 234 and ultimately permeability transition.

235 Mitochondria are the structural and functional elements of cell respiration. Cell  
 236 respiration is the reduction of oxygen by electron transfer coupled to electrochemical proton  
 237 translocation across the mtIM. In the process of oxidative phosphorylation (OXPHOS), the  
 238 catabolic reaction of oxygen consumption is electrochemically coupled to the transformation of  
 239 energy in the form of adenosine triphosphate (ATP; Mitchell 1961, 2011). Mitochondria are the  
 240 powerhouses of the cell which contain the machinery of the OXPHOS-pathways, including  
 241 transmembrane respiratory complexes (proton pumps with FMN, Fe-S and cytochrome *b, c,*  
 242 *aa<sub>3</sub>* redox systems); alternative dehydrogenases and oxidases; the coenzyme ubiquinone (Q);  
 243 F-ATPase or ATP synthase; the enzymes of the tricarboxylic acid cycle, fatty acid and  
 244 aminoacid oxidation; transporters of ions, metabolites and co-factors; and mitochondrial  
 245 kinases related to energy transfer pathways. The mitochondrial proteome comprises over 1,200  
 246 proteins (Calvo *et al.* 2015; 2017), mostly encoded by nuclear DNA (nDNA), with a variety of  
 247 functions, many of which are relatively well known (*e.g.*, proteins regulating mitochondrial  
 248 biogenesis or apoptosis), while others are still under investigation, or need to be identified (*e.g.*,  
 249 alanine transporter).

250 There is a constant crosstalk between mitochondria and the other cellular components.  
 251 The crosstalk between mitochondria and endoplasmic reticulum is involved in the regulation of  
 252 calcium homeostasis, cell division, autophagy, differentiation, anti-viral signaling (Murley and  
 253 Nunnari 2016). Mitochondria contribute to the formation of peroxisomes, which are hybrids of  
 254 mitochondrial and ER-derived precursors (Sugiura *et al.* 2017). Cellular mitochondrial  
 255 homeostasis (mitostasis) is maintained through regulation at both the transcriptional and post-  
 256 translational level. Cell signalling modules contribute to homeostatic regulation throughout the  
 257 cell cycle or even cell death by activating proteostatic modules (*e.g.*, the ubiquitin-proteasome  
 258 and autophagy-lysosome pathways) and genome stability modules in response to varying  
 259 energy demands and stress cues (Quiros *et al.* 2016).

260 Mitochondria typically maintain several copies of their own genome known as  
 261 mitochondrial DNA (mtDNA; hundred to thousands per cell; Cummins 1998), which is  
 262 maternally inherited. Biparental mitochondrial inheritance is documented in mammals, birds,  
 263 fish, reptiles and invertebrate groups, and is even the norm in bivalves (Breton *et al.* 2007;  
 264 White *et al.* 2008). mtDNA is compact (16.5 kB in humans) and encodes 13 protein subunits  
 265 of the transmembrane respiratory Complexes CI, CIII, CIV and F-ATPase, 22 tRNAs, and two  
 266 RNAs. Additional gene content has been suggested to include microRNAs, piRNA,  
 267 smithRNAs, repeat associated RNA, and even additional proteins (Duarte *et al.* 2014; Lee *et*  
 268 *al.* 2015; Cobb *et al.* 2016). The mitochondrial genome requires nuclear-encoded mitochondrial  
 269 targeted proteins for its maintenance and expression (Rackham *et al.* 2012).

270 Abbreviation: mt, as generally used in mtDNA. Mitochondrion is singular and  
 271 mitochondria is plural.

272 *‘For the physiologist, mitochondria afforded the first opportunity for an experimental*  
 273 *approach to structure-function relationships, in particular those involved in active transport,*  
 274 *vectorial metabolism, and metabolic control mechanisms on a subcellular level’* (Ernster and  
 275 Schatz 1981).

276

277

278

## 279 1. Introduction

280

281 Mitochondria are the powerhouses of the cell with numerous physiological, molecular,  
 282 and genetic functions (**Box 1**). Every study of mitochondrial health and disease is faced with  
 283 **E**volution, **A**ge, **G**ender and sex, **L**ifestyle, and **E**nvironment (EAGLE) as essential background

284 conditions intrinsic to the individual patient or subject, cohort, species, tissue and to some extent  
285 even cell line. As a large and coordinated group of laboratories and researchers, the mission of  
286 the global MitoEAGLE Network is to generate the necessary scale, type, and quality of  
287 consistent data sets and conditions to address this intrinsic complexity. Harmonization of  
288 experimental protocols and implementation of a quality control and data management system  
289 are required to interrelate results gathered across a spectrum of studies and to generate a  
290 rigorously monitored database focused on mitochondrial respiratory function. In this way,  
291 researchers within the same and across different disciplines will be positioned to compare  
292 findings across traditions and generations to an agreed upon set of clearly defined and accepted  
293 international standards.

294 Reliability and comparability of quantitative results depend on the accuracy of  
295 measurements under strictly-defined conditions. A conceptual framework is required to warrant  
296 meaningful interpretation and comparability of experimental outcomes carried out by research  
297 groups at different institutes. With an emphasis on quality of research, collected data can be  
298 useful far beyond the specific question of a particular experiment. Enabling meta-analytic  
299 studies is the most economic way of providing robust answers to biological questions (Cooper  
300 *et al.* 2009). Vague or ambiguous jargon can lead to confusion and may relegate valuable  
301 signals to wasteful noise. For this reason, measured values must be expressed in standard units  
302 for each parameter used to define mitochondrial respiratory function. Harmonization of  
303 nomenclature and definition of technical terms are essential to improve the awareness of the  
304 intricate meaning of current and past scientific vocabulary, for documentation and integration  
305 into databases in general, and quantitative modelling in particular (Beard 2005). The focus on  
306 coupling states and fluxes through metabolic pathways of aerobic energy transformation in  
307 mitochondrial preparations is a first step in the attempt to generate a conceptually-oriented  
308 nomenclature in bioenergetics and mitochondrial physiology. Coupling states of intact cells,  
309 the protonmotive force, and respiratory control by fuel substrates and specific inhibitors of  
310 respiratory enzymes will be reviewed in subsequent communications.

311  
312

## 313 **2. Oxidative phosphorylation and coupling states in mitochondrial preparations**

314 *‘Every professional group develops its own technical jargon for talking about matters of*  
315 *critical concern ... People who know a word can share that idea with other members of*  
316 *their group, and a shared vocabulary is part of the glue that holds people together and*  
317 *allows them to create a shared culture’ (Miller 1991).*

318

319 **Mitochondrial preparations** are defined as either isolated mitochondria, or tissue and  
320 cellular preparations in which the barrier function of the plasma membrane is disrupted. Since  
321 this entails the loss of cell viability, mitochondrial preparations are not studied *in vivo*. In  
322 contrast to isolated mitochondria and tissue homogenate preparations, mitochondria in  
323 permeabilized tissues and cells are *in situ* relative to the plasma membrane. The plasma  
324 membrane separates the intracellular compartment including the cytosol, nucleus, and  
325 organelles from the environment of the cell. The plasma membrane consists of a lipid bilayer,  
326 embedded proteins, and attached organic molecules that collectively control the selective  
327 permeability of ions, organic molecules, and particles across the cell boundary. The intact  
328 plasma membrane prevents the passage of many water-soluble mitochondrial substrates and  
329 inorganic ions—such as succinate, adenosine diphosphate (ADP) and inorganic phosphate (P<sub>i</sub>),  
330 that must be controlled at kinetically-saturating concentrations for the analysis of respiratory  
331 capacities; this limits the scope of investigations into mitochondrial respiratory function in  
332 intact cells.

333 The cholesterol content of the plasma membrane is high compared to mitochondrial  
334 membranes. Therefore, mild detergents—such as digitonin and saponin—can be applied to

335 selectively permeabilize the plasma membrane by interaction with cholesterol and allow free  
336 exchange of organic molecules and inorganic ions between the cytosol and the immediate cell  
337 environment, while maintaining the integrity and localization of organelles, cytoskeleton, and  
338 the nucleus. Application of optimum concentrations of permeabilization agents (mild detergents  
339 or toxins) leads to washout of cytosolic marker enzymes—such as lactate dehydrogenase—and  
340 results in the complete loss of cell viability, tested by nuclear staining using membrane-  
341 impermeable dyes, while mitochondrial function remains intact. Respiration of isolated  
342 mitochondria remains unaltered after the addition of low concentrations of digitonin or saponin.  
343 In addition to mechanical cell disruption during homogenization of tissue, permeabilization  
344 agents may be applied to ensure permeabilization of all cells. Suspensions of cells  
345 permeabilized in the respiration chamber and crude tissue homogenates contain all components  
346 of the cell at highly dilute concentrations. All mitochondria are retained in chemically-  
347 permeabilized mitochondrial preparations and crude tissue homogenates. In the preparation of  
348 isolated mitochondria, the cells or tissues are homogenized, and the mitochondria are separated  
349 from other cell fractions and purified by differential centrifugation, entailing the loss of a  
350 fraction of the total mitochondrial content. Typical mitochondrial recovery ranges from 30% to  
351 80%. Maximization of the purity of isolated mitochondria may compromise not only the  
352 mitochondrial yield but also the structural and functional integrity. Therefore, protocols to  
353 isolate mitochondria need to be optimized according to each study. The term mitochondrial  
354 preparation does not include further fractionation of mitochondrial components, neither  
355 submitochondrial particles.

356

### 357 *2.1. Respiratory control and coupling*

358

359 Respiratory coupling control states are established in studies of mitochondrial  
360 preparations to obtain reference values for various output variables. Physiological conditions *in*  
361 *vivo* deviate from these experimentally obtained states. Since kinetically-saturating  
362 concentrations, *e.g.*, of ADP or oxygen (O<sub>2</sub>; dioxygen), may not apply to physiological  
363 intracellular conditions, relevant information is obtained in studies of kinetic responses to  
364 variations in [ADP] or [O<sub>2</sub>] in the range between kinetically-saturating concentrations and  
365 anoxia (Gnaiger 2001).

366 **The steady-state:** Mitochondria represent a thermodynamically open system in non-  
367 equilibrium states of biochemical energy transformation. State variables (protonmotive force;  
368 redox states) and metabolic *rates* (fluxes) are measured in defined mitochondrial respiratory  
369 *states*. Steady-states can be obtained only in open systems, in which changes by *internal*  
370 transformations, *e.g.*, O<sub>2</sub> consumption, are instantaneously compensated for by *external* fluxes,  
371 *e.g.*, O<sub>2</sub> supply, preventing a change of O<sub>2</sub> concentration in the system (Gnaiger 1993b).  
372 Mitochondrial respiratory states monitored in closed systems satisfy the criteria of pseudo-  
373 steady states for limited periods of time, when changes in the system (concentrations of O<sub>2</sub>, fuel  
374 substrates, ADP, P<sub>i</sub>, H<sup>+</sup>) do not exert significant effects on metabolic fluxes (respiration,  
375 phosphorylation). Such pseudo-steady states require respiratory media with sufficient buffering  
376 capacity and substrates maintained at kinetically-saturating concentrations, and thus depend on  
377 the kinetics of the processes under investigation.

378 **Specification of biochemical dose:** Substrates, uncouplers, inhibitors, and other  
379 chemical reagents are titrated to dissect mitochondrial function. Nominal concentrations of  
380 these substances are usually reported as initial amount of substance concentration [mol·L<sup>-1</sup>] in  
381 the incubation medium. When aiming at the measurement of kinetically saturated processes—  
382 such as OXPHOS-capacities, the concentrations for substrates can be chosen according to the  
383 apparent equilibrium constant,  $K_m'$ . In the case of hyperbolic kinetics, only 80% of maximum  
384 respiratory capacity is obtained at a substrate concentration of four times the  $K_m'$ , whereas  
385 substrate concentrations of 5, 9, 19 and 49 times the  $K_m'$  are theoretically required for reaching



386 83%, 90%, 95% or 98% of the maximal rate (Gnaiger 2001). Other reagents are chosen to  
 387 inhibit or alter some processes. The amount of these chemicals in an experimental incubation  
 388 is selected to maximize effect, avoiding unacceptable off-target consequences that would  
 389 adversely affect the data being sought. Specifying the amount of substance in an incubation as  
 390 nominal concentration in the aqueous incubation medium can be ambiguous (Doskey *et al.*  
 391 2015), particularly for lipophilic substances (oligomycin, uncouplers, permeabilization agents)  
 392 or cations (TPP<sup>+</sup>; fluorescent dyes such as safranin, TMRM), which accumulate in biological  
 393 membranes or in the mitochondrial matrix. For example, a dose of digitonin of 8 fmol·cell<sup>-1</sup> (10  
 394 pg·cell<sup>-1</sup>; 10 µg·10<sup>-6</sup> cells) is optimal for permeabilization of endothelial cells, and the  
 395 concentration in the incubation medium has to be adjusted according to the cell density applied  
 396 (Doerrier *et al.* 2018).

397 Generally, dose/exposure can be specified per unit of biological sample, *i.e.*, (nominal  
 398 moles of xenobiotic)/(number of cells) [mol·cell<sup>-1</sup>] or, as appropriate, per mass of biological  
 399 sample [mol·kg<sup>-1</sup>]. This approach to specification of dose/exposure provides a scalable  
 400 parameter that can be used to design experiments, help interpret a wide variety of experimental  
 401 results, and provide absolute information that allows researchers worldwide to make the most  
 402 use of published data (Doskey *et al.* 2015).

403 **Phosphorylation, P<sup>»</sup>, and P<sup>»</sup>/O<sub>2</sub> ratio:** *Phosphorylation* in the context of OXPHOS is  
 404 defined as phosphorylation of ADP by P<sub>i</sub> to form ATP. On the other hand, the term  
 405 phosphorylation is used generally in many contexts, *e.g.*, protein phosphorylation. This justifies  
 406 consideration of a symbol more discriminating and specific than P as used in the P/O ratio  
 407 (phosphate to atomic oxygen ratio), where P indicates phosphorylation of ADP to ATP or GDP  
 408 to GTP (**Fig. 1**). We propose the symbol P<sup>»</sup> for the endergonic (uphill) direction of  
 409 phosphorylation ADP→ATP, and likewise the symbol P<sup>«</sup> for the corresponding exergonic  
 410 (downhill) hydrolysis ATP→ADP (**Fig. 2**). P<sup>»</sup> refers mainly to electrontransfer  
 411 phosphorylation but may also involve substrate-level phosphorylation as part of the  
 412 tricarboxylic acid (TCA) cycle (succinyl-CoA ligase; phosphoglycerate kinase) and  
 413 phosphorylation of ADP catalyzed by pyruvate kinase, and of GDP phosphorylated by  
 414 phosphoenolpyruvate carboxykinase. Transphosphorylation is performed by adenylate kinase,  
 415 creatine kinase, hexokinase and nucleoside diphosphate kinase. In isolated mammalian  
 416 mitochondria, ATP production catalyzed by adenylate kinase (2 ADP ↔ ATP + AMP) proceeds  
 417 without fuel substrates in the presence of ADP (Kömłódi and Tretter 2017). Kinase cycles are  
 418 involved in intracellular energy transfer and signal transduction for regulation of energy flux.

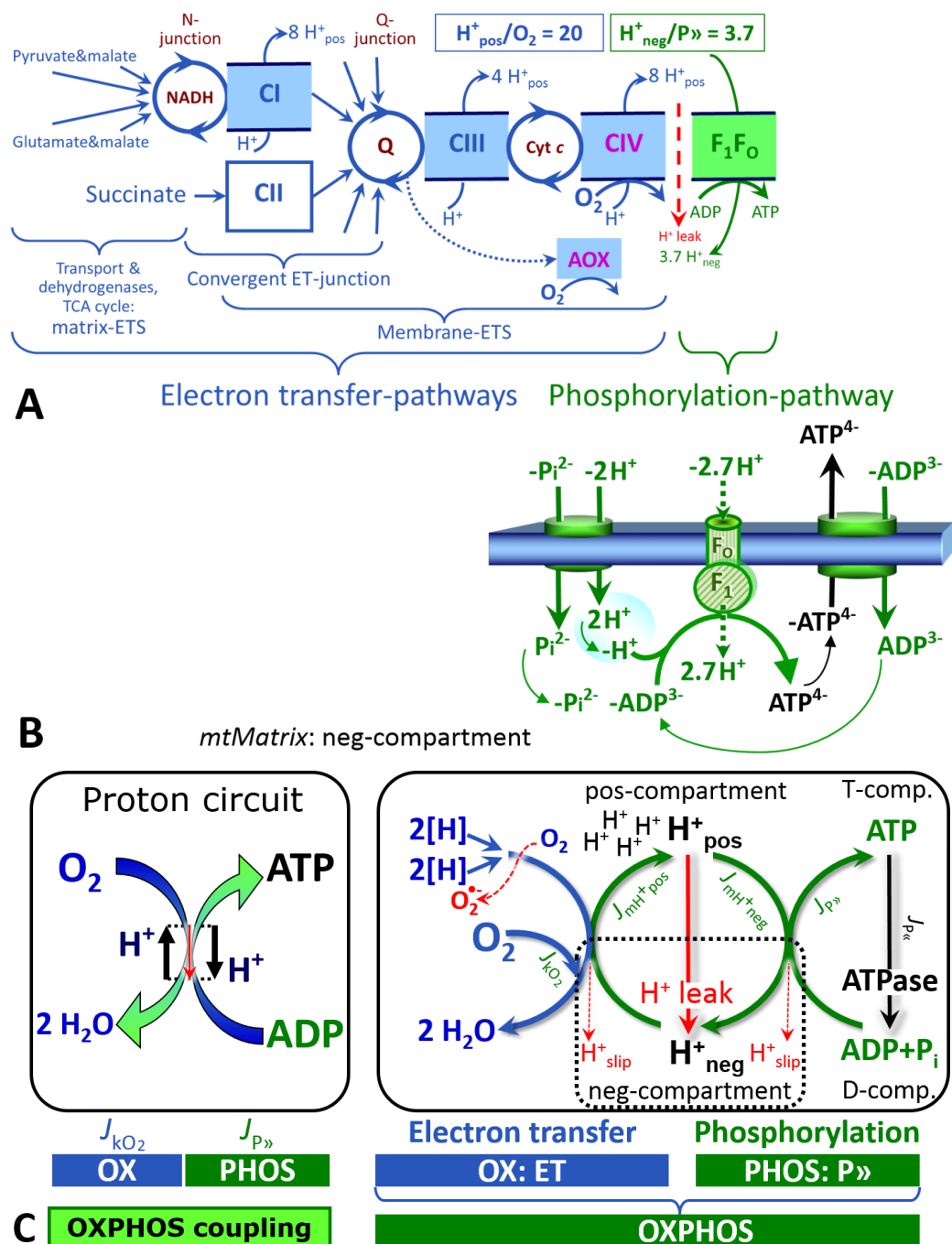
419 The P<sup>»</sup>/O<sub>2</sub> ratio (P<sup>»</sup>/4 e<sup>-</sup>) is two times the ‘P/O’ ratio (P<sup>»</sup>/2 e<sup>-</sup>) of classical bioenergetics.  
 420 P<sup>»</sup>/O<sub>2</sub> is a generalized symbol, not specific for determination of P<sub>i</sub> consumption (P<sub>i</sub>/O<sub>2</sub> flux  
 421 ratio), ADP depletion (ADP/O<sub>2</sub> flux ratio), or ATP production (ATP/O<sub>2</sub> flux ratio). The  
 422 mechanistic P<sup>»</sup>/O<sub>2</sub> ratio—or P<sup>»</sup>/O<sub>2</sub> stoichiometry—is calculated from the proton-to-O<sub>2</sub> and  
 423 proton-to-phosphorylation coupling stoichiometries (**Fig. 2A**):

$$424 \quad P^{\gg}/O_2 = \frac{H_{pos/O_2}^+}{H_{neg/P^{\gg}}^+} \quad (1)$$

425 The H<sup>+</sup><sub>pos</sub>/O<sub>2</sub> *coupling stoichiometry* (referring to the full 4 electron reduction of O<sub>2</sub>) depends  
 426 on the ET-pathway control state which defines the relative involvement of the three coupling  
 427 sites (CI, CIII and CIV) in the catabolic pathway of electrons to O<sub>2</sub>. This varies with: (1) a  
 428 bypass of CI by single or multiple electron input into the Q-junction; and (2) a bypass of CIV  
 429 by involvement of alternative oxidases, AOX, which are not expressed in mammalian  
 430 mitochondria.

431 H<sup>+</sup><sub>pos</sub>/O<sub>2</sub> is 12 in the ET-pathways involving CIII and CIV as proton pumps, increasing to  
 432 20 for the NADH-pathway (**Fig. 2A**), but a general consensus on H<sup>+</sup><sub>pos</sub>/O<sub>2</sub> stoichiometries  
 433 remains to be reached (Hinkle 2005; Wikström and Hummer 2012; Sazanov 2015). The  
 434 H<sup>+</sup><sub>neg</sub>/P<sup>»</sup> coupling stoichiometry (3.7; **Fig. 2A**) is the sum of 2.7 H<sup>+</sup><sub>neg</sub> required by the F-ATPase  
 435 of vertebrate and most invertebrate species (Watt *et al.* 2010) and the proton balance in the

436 translocation of ADP, ATP and  $P_i$  (Fig. 2B). Taken together, the mechanistic  $P_{\gg}/O_2$  ratio is  
 437 calculated at 5.4 and 3.3 for NADH- and succinate-linked respiration, respectively (Eq. 1). The  
 438 corresponding classical  $P_{\gg}/O$  ratios (referring to the 2 electron reduction of  $0.5 O_2$ ) are 2.7 and  
 439 1.6 (Watt *et al.* 2010), in agreement with the measured  $P_{\gg}/O$  ratio for succinate of  $1.58 \pm 0.02$   
 440 (Gnaiger *et al.* 2000).  
 441



442  
 443 **Fig. 2. Oxidative phosphorylation (OXPHOS).** (A) The mitochondrial electron transfer  
 444 system (ETS) is fuelled by diffusion and transport of substrates across the mtOM and mtIM and  
 445 consists of the matrix-ETS and membrane-ETS. ET-pathways are coupled to the  
 446 phosphorylation-pathway. ET-pathways converge at the N-junction and Q-junction. Additional  
 447 arrows indicate electron entry into the Q-junction through electron transferring flavoprotein,  
 448 glycerophosphate dehydrogenase, dihydro-orotate dehydrogenase, choline dehydrogenase, and  
 449 sulfide-ubiquinone oxidoreductase. The dotted arrow indicates the branched pathway of oxygen

450 consumption by alternative quinol oxidase (AOX). The  $H^+_{\text{pos}}/O_2$  ratio is the outward proton  
 451 flux from the matrix space to the positively (pos) charged compartment, divided by catabolic  
 452  $O_2$  flux in the NADH-pathway. The  $H^+_{\text{neg}}/P_{\gg}$  ratio is the inward proton flux from the inter-  
 453 membrane space to the negatively (neg) charged matrix space, divided by the flux of  
 454 phosphorylation of ADP to ATP. These are not fixed stoichiometries due to ion leaks and proton  
 455 slip. (B) Phosphorylation-pathway catalyzed by the proton pump  $F_1F_0$ -ATPase (F-ATPase,  
 456 ATP synthase), adenine nucleotide translocase, and inorganic phosphate transporter. The  
 457  $H^+_{\text{neg}}/P_{\gg}$  stoichiometry is the sum of the coupling stoichiometry in the F-ATPase reaction ( $-2.7$   
 458  $H^+_{\text{pos}}$  from the positive intermembrane space,  $2.7 H^+_{\text{neg}}$  to the matrix, *i.e.*, the negative  
 459 compartment) and the proton balance in the translocation of  $ADP^{2-}$ ,  $ATP^{3-}$  and  $P_i^{2-}$ . (C) The  
 460 proton circuit and coupling in OXPHOS.  $2[H]$  indicates the reduced hydrogen equivalents of  
 461 fuel substrates of the catabolic reaction  $k$  with oxygen.  $O_2$  flux,  $J_{kO_2}$ , through the catabolic ET-  
 462 pathway, is coupled to flux through the phosphorylation-pathway of ADP to ATP,  $J_{P_{\gg}}$ . The  
 463 proton pumps of the ET-pathway drive proton flux into the positive (pos) compartment,  $J_{mH^+pos}$ ,  
 464 generating the output protonmotive force (motive, subscript m). F-ATPase is coupled to inward  
 465 proton current into the negative (neg) compartment,  $J_{mH^+neg}$ , to phosphorylate  $ADP+P_i$  to ATP.  
 466 The system defined by the boundaries (full black line) is not a black box, but is analysed as a  
 467 compartmental system. The negative compartment (neg-compartment, enclosed by the dotted  
 468 line) is the matrix space, separated by the mtIM from the positive compartment (pos-  
 469 compartment).  $ADP+P_i$  and ATP are the substrate- and product-compartments (scalar ADP and  
 470 ATP compartments, D-comp. and T-comp.), respectively. At steady-state proton turnover,  
 471  $J_{\infty H^+}$ , and ATP turnover,  $J_{\infty P}$ , maintain concentrations constant, when  $J_{mH^+\infty} = J_{mH^+pos} = J_{mH^+neg}$ ,  
 472 and  $J_{P_{\infty}} = J_{P_{\gg}} = J_{P_{\ll}}$ . Modified from (A) Lemieux *et al.* (2017) and (B,C) Gnaiger (2014).

473  
 474 The effective  $P_{\gg}/O_2$  flux ratio ( $Y_{P_{\gg}/O_2} = J_{P_{\gg}}/J_{kO_2}$ ) is diminished relative to the mechanistic  
 475  $P_{\gg}/O_2$  ratio by intrinsic and extrinsic uncoupling and dyscoupling (Fig. 3). Such generalized  
 476 uncoupling is different from switching to mitochondrial pathways that involve fewer than three  
 477 proton pumps ('coupling sites': Complexes CI, CIII and CIV), bypassing CI through multiple  
 478 electron entries into the Q-junction, or CIII and CIV through AOX (Fig. 2). Reprogramming of  
 479 mitochondrial pathways may be considered as a switch of gears (changing the stoichiometry)  
 480 rather than uncoupling (loosening the stoichiometry). In addition,  $Y_{P_{\gg}/O_2}$  depends on several  
 481 experimental conditions of flux control, increasing as a hyperbolic function of  $[ADP]$  to a  
 482 maximum value (Gnaiger 2001).

483 **Control and regulation:** The terms metabolic *control* and *regulation* are frequently used  
 484 synonymously, but are distinguished in metabolic control analysis: 'We could understand the  
 485 regulation as the mechanism that occurs when a system maintains some variable constant over  
 486 time, in spite of fluctuations in external conditions (homeostasis of the internal state). On the  
 487 other hand, metabolic control is the power to change the state of the metabolism in response to  
 488 an external signal' (Fell 1997). Respiratory control may be induced by experimental control  
 489 signals that *exert* an influence on: (1) ATP demand and ADP phosphorylation-rate; (2) fuel  
 490 substrate composition, pathway competition; (3) available amounts of substrates and  $O_2$ , *e.g.*,  
 491 starvation and hypoxia; (4) the protonmotive force, redox states, flux-force relationships,  
 492 coupling and efficiency; (5)  $Ca^{2+}$  and other ions including  $H^+$ ; (6) inhibitors, *e.g.*, nitric oxide  
 493 or intermediary metabolites such as oxaloacetate; (7) signalling pathways and regulatory  
 494 proteins, *e.g.*, insulin resistance, transcription factor hypoxia inducible factor 1. *Mechanisms* of  
 495 respiratory control and regulation include adjustments of: (1) enzyme activities by allosteric  
 496 mechanisms and phosphorylation; (2) enzyme content, concentrations of cofactors and  
 497 conserved moieties—such as adenylates, nicotinamide adenine dinucleotide [ $NAD^+/NADH$ ],  
 498 coenzyme Q, cytochrome *c*; (3) metabolic channeling by supercomplexes; and (4)  
 499 mitochondrial density (enzyme concentrations and membrane area) and morphology (cristae  
 500 folding, fission and fusion). Mitochondria are targeted directly by hormones, thereby affecting

501 their energy metabolism (Lee *et al.* 2013; Gerö and Szabo 2016; Price and Dai 2016; Moreno  
 502 *et al.* 2017). Evolutionary or acquired differences in the genetic and epigenetic basis of  
 503 mitochondrial function (or dysfunction) between subjects and gene therapy; age; gender,  
 504 biological sex, and hormone concentrations; life style including exercise and nutrition; and  
 505 environmental issues including thermal, atmospheric, toxicological and pharmacological  
 506 factors, exert an influence on all control mechanisms listed above. For reviews, see Brown  
 507 1992; Gnaiger 1993a, 2009; 2014; Paradies *et al.* 2014; Morrow *et al.* 2017.

508 **Respiratory control and response:** Lack of control by a metabolic pathway, *e.g.*,  
 509 phosphorylation-pathway, means that there will be no response to a variable activating it, *e.g.*,  
 510 [ADP]. The reverse, however, is not true as the absence of a response to [ADP] does not exclude  
 511 the phosphorylation-pathway from having some degree of control. The degree of control of a  
 512 component of the OXPHOS-pathway on an output variable—such as O<sub>2</sub> flux, will in general  
 513 be different from the degree of control on other outputs—such as phosphorylation-flux or  
 514 proton leak flux. Therefore, it is necessary to be specific as to which input and output are under  
 515 consideration (Fell 1997).

516 **Respiratory coupling control and ET-pathway control:** Respiratory control refers to  
 517 the ability of mitochondria to adjust O<sub>2</sub> flux in response to external control signals by engaging  
 518 various mechanisms of control and regulation. Respiratory control is monitored in a  
 519 mitochondrial preparation under conditions defined as respiratory states. When  
 520 phosphorylation of ADP to ATP is stimulated or depressed, an increase or decrease is observed  
 521 in electron transfer measured as O<sub>2</sub> flux in respiratory coupling states of intact mitochondria  
 522 ('controlled states' in the classical terminology of bioenergetics). Alternatively, coupling of  
 523 electron transfer with phosphorylation is disengaged by uncouplers. These protonophores are  
 524 weak lipid-soluble acids which disrupt the barrier function of the mtIM and thus shortcircuit  
 525 the protonmotive system, functioning like a clutch in a mechanical system. The corresponding  
 526 coupling control state is characterized by a high O<sub>2</sub> flux without control by P» ('uncontrolled  
 527 state').

528 ET-pathway control states are obtained in mitochondrial preparations by depletion of  
 529 endogenous substrates and addition to the mitochondrial respiration medium of fuel substrates  
 530 (CHNO; 2[H] in **Fig. 2C**) and specific inhibitors, activating selected mitochondrial catabolic  
 531 pathways, k (**Fig. 2A**). Coupling control states and pathway control states are complementary,  
 532 since mitochondrial preparations depend on an exogenous supply of pathway-specific fuel  
 533 substrates and oxygen (Gnaiger 2014).

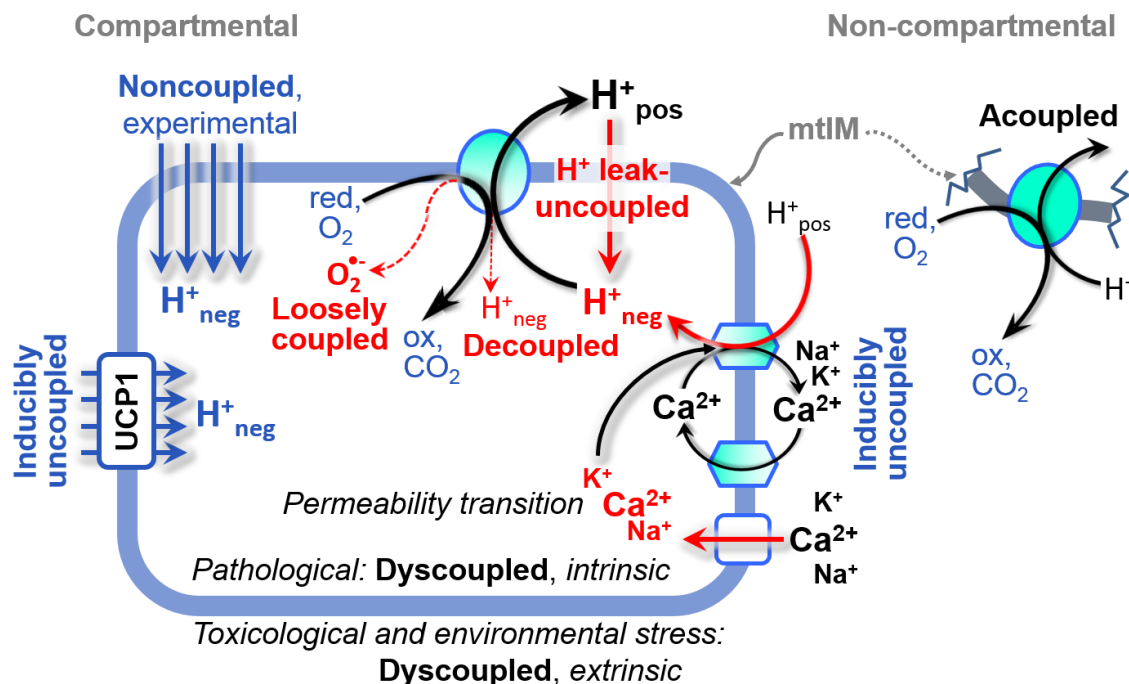
534 **Coupling:** In mitochondrial electron transfer, vectorial transmembrane proton flux is  
 535 coupled through the proton pumps CI, CIII and CIV to the catabolic flux of scalar reactions,  
 536 collectively measured as O<sub>2</sub> flux (**Fig. 2**). Thus mitochondria are elements of energy  
 537 transformation. Energy cannot be lost or produced in any internal process (First Law of  
 538 thermodynamics). Open and closed systems can gain or lose energy only by external fluxes—  
 539 by exchange with the environment. Energy is a conserved quantity. Therefore, energy can  
 540 neither be produced by mitochondria, nor is there any internal process without energy  
 541 conservation. Exergy is defined as the 'free energy' with the potential to perform work.  
 542 *Coupling* is the mechanistic linkage of an exergonic process (spontaneous, negative exergy  
 543 change) with an endergonic process (positive exergy change) in energy transformations which  
 544 conserve part of the exergy that would be irreversibly lost or dissipated in an uncoupled process.

545 **Uncoupling:** Uncoupling of mitochondrial respiration is a general term comprising  
 546 diverse mechanisms:

- 547 1. Proton leak across the mtIM from the pos- to the neg-compartment (**Fig. 2C**);
- 548 2. Cycling of other cations, strongly stimulated by permeability transition, or  
 549 experimentally induced by valinomycin in the presence of K<sup>+</sup>;
- 550 3. Proton slip in the proton pumps when protons are effectively not pumped (CI, CIII and  
 551 CIV) or are not driving phosphorylation (F-ATPase);



- 552 4. Loss of compartmental integrity when electron transfer is acoupled;  
 553 5. Electron leak in the loosely coupled univalent reduction of O<sub>2</sub> to superoxide (O<sub>2</sub><sup>•-</sup>;  
 554 superoxide anion radical).



555 **Fig 3. Mechanisms of respiratory uncoupling.** An intact mitochondrial inner membrane,  
 556 mtIM, is required for vectorial, compartmental coupling. 'Acoupled' respiration is the  
 557 consequence of structural disruption with catalytic activity of non-compartmental  
 558 mitochondrial fragments. Inducibly uncoupled (activation of UCP1) and experimentally  
 559 noncoupled respiration (titration of protonophores) stimulate respiration to maximum O<sub>2</sub> flux.  
 560 H<sup>+</sup> leak-uncoupled, decoupled, and loosely coupled respiration are components of intrinsic  
 561 uncoupling. Pathological dysfunction may affect all types of uncoupling, including  
 562 permeability transition, causing intrinsically dyscoupled respiration. Similarly, toxicological  
 563 and environmental stress factors can cause extrinsically dyscoupled respiration.

565 Differences of terms—uncoupled vs. noncoupled—are easily overlooked, although they relate  
 566 to different meanings of uncoupling (**Fig. 3**).

## 569 2.2. Coupling states and respiratory rates

571 **Respiratory capacities in coupling control states:** To extend the classical nomenclature  
 572 on mitochondrial coupling states (Section 2.3) by a concept-driven terminology that  
 573 incorporates explicitly information on the meaning of respiratory states, the terminology must  
 574 be general and not restricted to any particular experimental protocol or mitochondrial  
 575 preparation (Gnaiger 2009). Concept-driven nomenclature aims at mapping the *meaning and*  
 576 *concept behind* the words and acronyms onto the *forms* of words and acronyms (Miller 1991).  
 577 The focus of concept-driven nomenclature is primarily the conceptual 'why', along with  
 578 clarification of the experimental 'how'. Respiratory capacities delineate, comparable to channel  
 579 capacity in information theory (Schneider 2006), the upper bound of the rate of respiration  
 580 measured in defined coupling control states and electron transfer-pathway (ET-pathway) states  
 581 (**Fig. 4**).

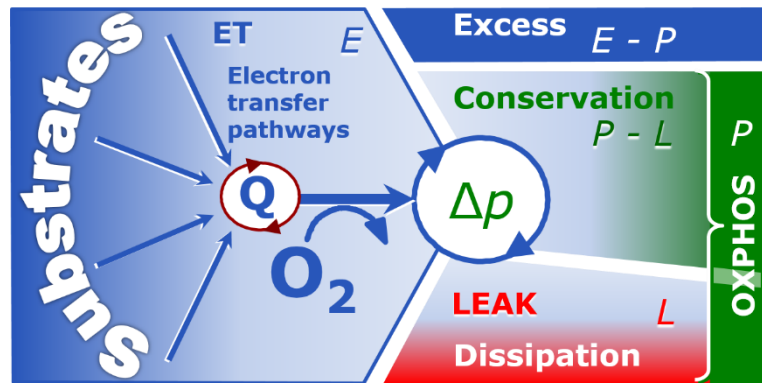
582 To provide a diagnostic reference for respiratory capacities of core energy metabolism,  
 583 the capacity of *oxidative phosphorylation*, OXPHOS, is measured at kinetically-saturating  
 584 concentrations of ADP and P<sub>i</sub>. The *oxidative ET-capacity* reveals the limitation of OXPHOS-



585 capacity mediated by the *phosphorylation*-pathway. The ET- and phosphorylation-pathways  
 586 comprise coupled segments of the OXPHOS-system. ET-capacity is measured as noncoupled  
 587 respiration by application of *external uncouplers*. The contribution of *intrinsically uncoupled*  
 588 O<sub>2</sub> consumption is studied by preventing the stimulation of phosphorylation either in the  
 589 absence of ADP or by inhibition of the phosphorylation-pathway. The corresponding states are  
 590 collectively classified as LEAK-states, when O<sub>2</sub> consumption compensates mainly for ion  
 591 leaks, including the proton leak. Defined coupling states are induced by: (1) adding cation  
 592 chelators such as EGTA, binding free Ca<sup>2+</sup> and thus limiting cation cycling; (2) adding ADP  
 593 and P<sub>i</sub>; (3) inhibiting the phosphorylation-pathway; and (4) uncoupler titrations, while  
 594 maintaining a defined ET-pathway state with constant fuel substrates and inhibitors of specific  
 595 branches of the ET-pathway (Fig. 2A).

597 **Fig. 4. Four-compartment**  
 598 **model of oxidative**  
 599 **phosphorylation.**

600 Respiratory states (ET, OXPHOS, LEAK; **Table 1**) and corresponding rates ( $E$ ,  $P$ ,  $L$ ) are connected by the  
 601 protonmotive force,  $\Delta p$ . ET-capacity,  $E$ , is partitioned into (1) dissipative LEAK-respiration,  $L$ ,  
 602 when the Gibbs energy change of catabolic O<sub>2</sub> flux is irreversibly  
 603 lost, (2) net OXPHOS-capacity,  $P-L$ , with partial conservation of the capacity to perform work,  
 604 and (3) the excess capacity,  $E-P$ . Modified from Gnaiger (2014).



611 **Table 1. Coupling states and residual oxygen consumption in mitochondrial**  
 612 **preparations in relation to respiration- and phosphorylation-flux,  $J_{\text{KO}_2}$  and  $J_{\text{P}}$ ,**  
 613 **and protonmotive force,  $\Delta p$ .** Coupling states are established at kinetically-saturating  
 614 concentrations of fuel substrates and O<sub>2</sub>.

State	$J_{\text{KO}_2}$	$J_{\text{P}}$	$\Delta p$	Inducing factors	Limiting factors
LEAK	$L$ ; low, cation leak-dependent respiration	0	max.	proton leak, slip, and cation cycling	$J_{\text{P}} = 0$ : (1) without ADP, $L_N$ ; (2) max. ATP/ADP ratio, $L_T$ ; or (3) inhibition of the phosphorylation-pathway, $L_{\text{Omy}}$
OXPHOS	$P$ ; high, ADP-stimulated respiration	max.	high	kinetically-saturating [ADP] and [P <sub>i</sub> ]	$J_{\text{P}}$ by phosphorylation-pathway; or $J_{\text{KO}_2}$ by ET-capacity
ET	$E$ ; max., noncoupled respiration	0	low	optimal external uncoupler concentration for max. $J_{\text{O}_2, E}$	$J_{\text{KO}_2}$ by ET-capacity
ROX	$R_{\text{ox}}$ ; min., residual O <sub>2</sub> consumption	0	0	$J_{\text{O}_2, \text{Rox}}$ in non-ET-pathway oxidation reactions	full inhibition of ET-pathway; or absence of fuel substrates

616 The three coupling states,  
 617 ET, LEAK and OXPHOS, are  
 618 shown schematically with the  
 619 corresponding respiratory rates,  
 620 abbreviated as  $E$ ,  $L$  and  $P$ ,  
 621 respectively (Fig. 4). We  
 622 distinguish metabolic pathways  
 623 from metabolic states and the  
 624 corresponding metabolic rates;  
 625 for example: ET-pathways (Fig.  
 626 4), ET-states (Fig. 5C), and ET-  
 627 capacities,  $E$ , respectively (Table  
 628 1). The protonmotive force is  
 629 high in the OXPHOS-state when  
 630 it drives phosphorylation,  
 631 maximum in the LEAK-state of  
 632 coupled mitochondria, driven by  
 633 LEAK-respiration at a minimum  
 634 back flux of cations to the matrix  
 635 side, and very low in the ET-state  
 636 when uncouplers short-circuit the  
 637 proton cycle (Table 1).

638 **LEAK-state (Fig. 5A):**  
 639 The LEAK-state is defined as a  
 640 state of mitochondrial respiration  
 641 when  $O_2$  flux mainly  
 642 compensates for ion leaks in the  
 643 absence of ATP synthesis, at  
 644 kinetically-saturating  
 645 concentrations of  $O_2$  and  
 646 respiratory fuel substrates.  
 647 LEAK-respiration is measured to  
 648 obtain an estimate of *intrinsic*  
 649 *uncoupling* without addition of  
 650 an experimental uncoupler: (1)  
 651 in the absence of adenylates, *i.e.*,  
 652 AMP, ADP and ATP; (2) after  
 653 depletion of ADP at a maximum  
 654 ATP/ADP ratio; or (3) after  
 655 inhibition of the  
 656 phosphorylation-pathway by  
 657 inhibitors of F-ATPase—such as  
 658 oligomycin, or of adenine nucleotide  
 659 translocase—such as carboxyatractyloside. Adjustment  
 660 of the nominal concentration of these inhibitors to the density of biological sample applied can  
 661 minimize or avoid inhibitory side-effects exerted on ET-capacity or even some dyscoupling.

662 **Proton leak and uncoupled respiration:** Proton leak is a leak current of protons. The  
 663 intrinsic proton leak is the *uncoupled* process in which protons diffuse across the mtIM in the  
 664 dissipative direction of the downhill protonmotive force without coupling to phosphorylation  
 665 (Fig. 5A). The proton leak flux depends non-linearly on the protonmotive force (Garlid *et al.*  
 666 1989; Divakaruni and Brand 2011), it is a property of the mtIM and may be enhanced due to  
 possible contaminations by free fatty acids. Inducible uncoupling mediated by uncoupling

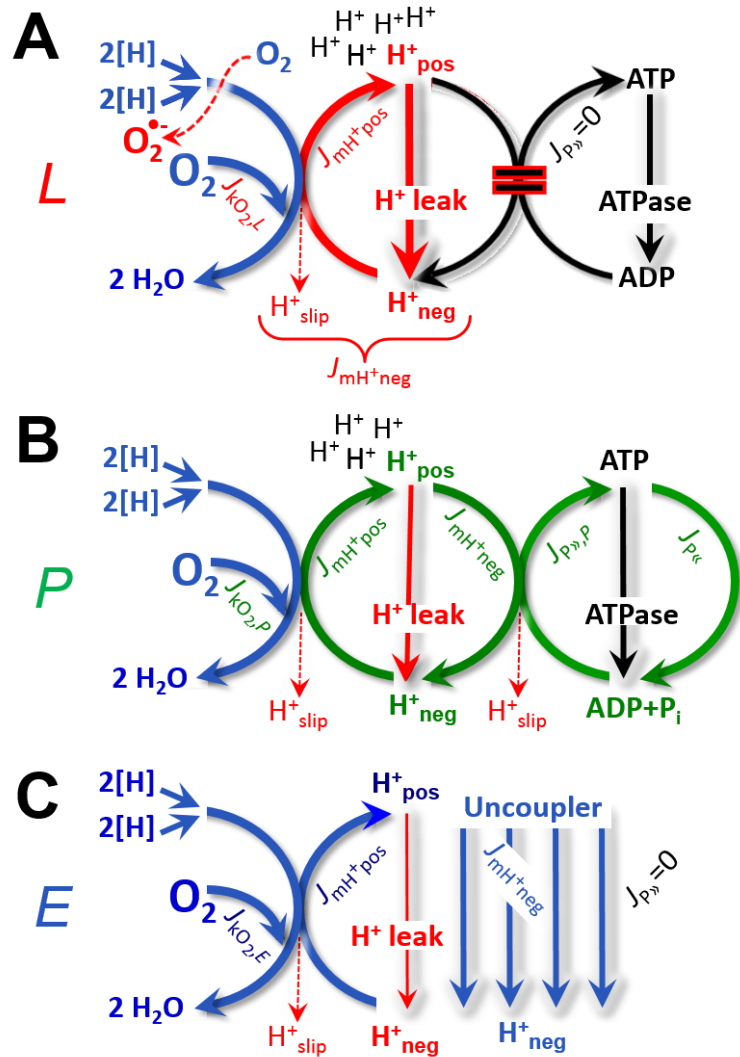


**Fig. 5. Respiratory coupling states. A: LEAK-state and rate,  $L$ :** Phosphorylation is arrested,  $J_{P>} = 0$ , and catabolic  $O_2$  flux,  $J_{kO_2,L}$ , is controlled mainly by the proton leak,  $J_{mH^+neg,L}$ , at maximum protonmotive force (Fig. 3). **B: OXPHOS-state and rate,  $P$ :** Phosphorylation,  $J_{P>}$ , is stimulated by kinetically-saturating  $[ADP]$  and  $[P_i]$ , and is supported by a high protonmotive force.  $O_2$  flux,  $J_{kO_2,P}$ , is well-coupled at a  $P>/O_2$  ratio of  $J_{P>,P}/J_{kO_2,P}$ . **C: ET-state and rate,  $E$ :** Noncoupled respiration,  $J_{kO_2,E}$ , is maximum at optimum exogenous uncoupler concentration and phosphorylation is zero,  $J_{P>} = 0$ . See also Fig. 2.

667 protein 1 (UCP1) is physiologically controlled, *e.g.*, in brown adipose tissue. UCP1 is a member  
 668 of the mitochondrial carrier family which is involved in the translocation of protons across the  
 669 mtIM (Klingenberg 2017). Consequently, the short-circuit diminishes the protonmotive force  
 670 and stimulates electron transfer to O<sub>2</sub> and heat dissipation without phosphorylation of ADP.

671 **Cation cycling:** There can be other cation contributors to leak current including calcium  
 672 and probably magnesium. Calcium current is balanced by mitochondrial Na<sup>+</sup>/Ca<sup>2+</sup> exchange,  
 673 which is balanced by Na<sup>+</sup>/H<sup>+</sup> or K<sup>+</sup>/H<sup>+</sup> exchanges. This is another effective uncoupling  
 674 mechanism different from proton leak (**Table 2**).

675

676

**Table 2. Terms on respiratory coupling and uncoupling.**

Term	$J_{\text{K}O_2}$	$P_{\gg}/O_2$	Note	
acoupled		0	electron transfer in mitochondrial fragments without vectorial proton translocation ( <b>Fig. 3</b> )	
intrinsic, no protonophore added	uncoupled	$L$	0	non-phosphorylating LEAK-respiration ( <b>Fig. 5A</b> )
	proton leak-uncoupled		0	component of $L$ , H <sup>+</sup> diffusion across the mtIM ( <b>Fig. 3</b> )
	decoupled		0	component of $L$ , proton slip ( <b>Fig. 3</b> )
	loosely coupled		0	component of $L$ , lower coupling due to superoxide formation and bypass of proton pumps ( <b>Fig. 3</b> )
	dyscoupled		0	pathologically, toxicologically, environmentally increased uncoupling, mitochondrial dysfunction
	inducibly uncoupled		0	by UCP1 or cation ( <i>e.g.</i> , Ca <sup>2+</sup> ) cycling ( <b>Fig. 3</b> )
noncoupled	$E$	0	non-phosphorylating respiration stimulated to maximum flux at optimum exogenous uncoupler concentration ( <b>Fig. 5C</b> )	
well-coupled	$P$	high	phosphorylating respiration with an intrinsic LEAK component ( <b>Fig. 5B</b> )	
fully coupled	$P - L$	max.	OXPHOS-capacity corrected for LEAK-respiration ( <b>Fig. 4</b> )	

677

678

679

680

681

682

683

684

685

686

**Proton slip and decoupled respiration:** Proton slip is the *decoupled* process in which protons are only partially translocated by a proton pump of the ET-pathways and slip back to the original compartment. The proton leak is the dominant contributor to the overall leak current in mammalian mitochondria incubated under physiological conditions at 37 °C, whereas proton slip is increased at lower experimental temperature (Canton *et al.* 1995). Proton slip can also happen in association with the F-ATPase, in which the proton slips downhill across the pump to the matrix without contributing to ATP synthesis. In each case, proton slip is a property of the proton pump and increases with the pump turnover rate.

687

688

689

690

691

692

693

**Electron leak and loosely coupled respiration:** Superoxide production by the ETS leads to a bypass of proton pumps and correspondingly lower  $P_{\gg}/O_2$  ratio. This depends on the actual site of electron leak and the scavenging of hydrogen peroxide by cytochrome *c*, whereby electrons may re-enter the ETS with proton translocation by CIV.

**Loss of compartmental integrity and acoupled respiration:** Electron transfer and catabolic O<sub>2</sub> flux proceed without compartmental proton translocation in disrupted mitochondrial fragments. Such fragments form during mitochondrial isolation, and may not fully fuse to re-establish structurally intact mitochondria. Loss of mtIM integrity, therefore, is

694 the cause of acoupled respiration, which is a nonvectorial dissipative process without control  
695 by the protonmotive force.

696 **Dyscoupled respiration:** Mitochondrial injuries may lead to *dyscoupling* as a  
697 pathological or toxicological cause of *uncoupled* respiration. Dyscoupling may involve any  
698 type of uncoupling mechanism, *e.g.*, opening the permeability transition pore. Dyscoupled  
699 respiration is distinguished from the experimentally induced *noncoupled* respiration in the ET-  
700 state (**Table 2**).

701 **OXPPOS-state (Fig. 5B):** The OXPPOS-state is defined as the respiratory state with  
702 kinetically-saturating concentrations of O<sub>2</sub>, respiratory and phosphorylation substrates, and  
703 absence of exogenous uncoupler, which provides an estimate of the maximal respiratory  
704 capacity in the OXPPOS-state for any given ET-pathway state. Respiratory capacities at  
705 kinetically-saturating substrate concentrations provide reference values or upper limits of  
706 performance, aiming at the generation of data sets for comparative purposes. Physiological  
707 activities and effects of substrate kinetics can be evaluated relative to the OXPPOS-capacity.

708 As discussed previously, 0.2 mM ADP does not fully saturate flux in isolated  
709 mitochondria (Gnaiger 2001; Puchowicz *et al.* 2004); greater ADP concentration is required,  
710 particularly in permeabilized muscle fibres and cardiomyocytes, to overcome limitations by  
711 intracellular diffusion and by the reduced conductance of the mtOM (Jepihhina *et al.* 2011,  
712 Illaste *et al.* 2012, Simson *et al.* 2016), either through interaction with tubulin (Rostovtseva *et al.*  
713 2008) or other intracellular structures (Birkedal *et al.* 2014). In permeabilized muscle fibre  
714 bundles of high respiratory capacity, the apparent  $K_m$  for ADP increases up to 0.5 mM (Saks *et al.*  
715 1998), consistent with experimental evidence that >90% saturation is reached only at >5  
716 mM ADP (Pesta and Gnaiger 2012). Similar ADP concentrations are also required for accurate  
717 determination of OXPPOS-capacity in human clinical cancer samples and permeabilized cells  
718 (Klepinin *et al.* 2016; Koit *et al.* 2017). Whereas 2.5 to 5 mM ADP is sufficient to obtain the  
719 actual OXPPOS-capacity in many types of permeabilized tissue and cell preparations,  
720 experimental validation is required in each specific case.

721 **Electron transfer-state (Fig. 5C):** The ET-state is defined as the *noncoupled* state with  
722 kinetically-saturating concentrations of O<sub>2</sub>, respiratory substrate and optimum *exogenous*  
723 uncoupler concentration for maximum O<sub>2</sub> flux. O<sub>2</sub> flux determined in the ET-state yields an  
724 estimate of ET-capacity. Inhibition of respiration is observed above optimum uncoupler  
725 concentrations. As a consequence of the nearly collapsed protonmotive force, the driving force  
726 is insufficient for phosphorylation, and  $J_{P_{\gg}} = 0$ .

727 **ROX state and Rox:** Besides the three fundamental coupling states of mitochondrial  
728 preparations, the state of residual O<sub>2</sub> consumption, ROX, is relevant to assess respiratory  
729 function. ROX is not a coupling state. The rate of residual oxygen consumption, *Rox*, is defined  
730 as O<sub>2</sub> consumption due to oxidative reactions measured after inhibition of ET—with rotenone,  
731 malonic acid and antimycin A. Cyanide and azide inhibit not only CIV but catalase and several  
732 peroxidases involved in *Rox*. However, high concentrations of antimycin A, but not rotenone  
733 or cyanide, inhibit peroxisomal acyl-CoA oxidase and D-amino acid oxidase (Vamecq *et al.*  
734 1987). ROX represents a baseline that is used to correct respiration in defined coupling states.  
735 *Rox* is not necessarily equivalent to non-mitochondrial reduction of O<sub>2</sub>, considering O<sub>2</sub>-  
736 consuming reactions in mitochondria that are not related to ET—such as O<sub>2</sub> consumption in  
737 reactions catalyzed by monoamine oxidases (type A and B), monooxygenases (cytochrome  
738 P450 monooxygenases), dioxygenase (sulfur dioxygenase and trimethyllysine dioxygenase),  
739 and several hydroxylases. Even isolated mitochondrial fractions, especially those obtained from  
740 liver, may be contaminated by peroxisomes. This fact makes the exact determination of  
741 mitochondrial O<sub>2</sub> consumption and mitochondria-associated generation of reactive oxygen  
742 species complicated (Schönfeld *et al.* 2009; Speijer 2016; **Fig. 1**). The dependence of ROX-  
743 linked O<sub>2</sub> consumption needs to be studied in detail together with non-ET enzyme activities,



744 availability of specific substrates, O<sub>2</sub> concentration, and electron leakage leading to the  
745 formation of reactive oxygen species.

746 **Quantitative relations:**  $E$  may exceed or be equal to  $P$ .  $E > P$  is observed in many types  
747 of mitochondria, varying between species, tissues and cell types (Gnaiger 2009).  $E - P$  is the  
748 excess ET-capacity pushing the phosphorylation-flux (**Fig. 2B**) to the limit of its *capacity of*  
749 *utilizing* the protonmotive force. In addition, the magnitude of  $E - P$  depends on the tightness of  
750 respiratory coupling or degree of uncoupling, since an increase of  $L$  causes  $P$  to increase  
751 towards the limit of  $E$ . The *excess*  $E - P$  capacity,  $E - P$ , therefore, provides a sensitive diagnostic  
752 indicator of specific injuries of the phosphorylation-pathway, under conditions when  $E$  remains  
753 constant but  $P$  declines relative to controls (**Fig. 4**). Substrate cocktails supporting simultaneous  
754 convergent electron transfer to the Q-junction for reconstitution of TCA cycle function establish  
755 pathway control states with high ET-capacity, and consequently increase the sensitivity of the  
756  $E - P$  assay.

757  $E$  cannot theoretically be lower than  $P$ .  $E < P$  must be discounted as an artefact, which  
758 may be caused experimentally by: (1) loss of oxidative capacity during the time course of the  
759 respirometric assay, since  $E$  is measured subsequently to  $P$ ; (2) using insufficient uncoupler  
760 concentrations; (3) using high uncoupler concentrations which inhibit ET (Gnaiger 2008); (4)  
761 high oligomycin concentrations applied for measurement of  $L$  before titrations of uncoupler,  
762 when oligomycin exerts an inhibitory effect on  $E$ . On the other hand, the excess ET-capacity is  
763 overestimated if non-saturating [ADP] or [P<sub>i</sub>] are used. See State 3 in the next section.

764 The net OXPHOS-capacity is calculated by subtracting  $L$  from  $P$  (**Fig. 4**). Then the net  
765  $P \gg O_2$  equals  $P \gg (P - L)$ , wherein the dissipative LEAK component in the OXPHOS-state may  
766 be overestimated. This can be avoided by measuring LEAK-respiration in a state when the  
767 protonmotive force is adjusted to its slightly lower value in the OXPHOS-state—by titration of  
768 an ET inhibitor (Divakaruni and Brand 2011). Any turnover-dependent components of proton  
769 leak and slip, however, are underestimated under these conditions (Garlid *et al.* 1993). In  
770 general, it is inappropriate to use the term *ATP production* or *ATP turnover* for the difference  
771 of O<sub>2</sub> flux measured in states  $P$  and  $L$ . The difference  $P - L$  is the upper limit of the part of  
772 OXPHOS-capacity that is freely available for ATP production (corrected for LEAK-  
773 respiration) and is fully coupled to phosphorylation with a maximum mechanistic stoichiometry  
774 (**Fig. 4**).

775

### 776 2.3. Classical terminology for isolated mitochondria

777 *'When a code is familiar enough, it ceases appearing like a code; one forgets that there*  
778 *is a decoding mechanism. The message is identical with its meaning'* (Hofstadter 1979).

779

780 Chance and Williams (1955; 1956) introduced five classical states of mitochondrial  
781 respiration and cytochrome redox states. **Table 3** shows a protocol with isolated mitochondria  
782 in a closed respirometric chamber, defining a sequence of respiratory states. States and rates  
783 are not specifically distinguished in this nomenclature.

784 **State 1** is obtained after addition of isolated mitochondria to air-saturated  
785 isoosmotic/isotonic respiration medium containing P<sub>i</sub>, but no fuel substrates and no adenylates,  
786 *i.e.*, AMP, ADP, ATP.

787 **State 2** is induced by addition of a 'high' concentration of ADP (typically 100 to 300  
788 μM), which stimulates respiration transiently on the basis of endogenous fuel substrates and  
789 phosphorylates only a small portion of the added ADP. State 2 is then obtained at a low  
790 respiratory activity limited by exhausted endogenous fuel substrate availability (**Table 3**). If  
791 addition of specific inhibitors of respiratory complexes—such as rotenone—does not cause a  
792 further decline of O<sub>2</sub> flux, State 2 is equivalent to the ROX state (See below.). If inhibition is  
793 observed, undefined endogenous fuel substrates are a confounding factor of pathway control,  
794 contributing to the effect of subsequently externally added substrates and inhibitors. In contrast



795 to the original protocol, an alternative sequence of titration steps is frequently applied, in which  
 796 the alternative ‘State 2’ has an entirely different meaning, when this second state is induced by  
 797 addition of fuel substrate without ADP (LEAK-state; in contrast to State 2 defined in **Table 1**  
 798 as a ROX state), followed by addition of ADP.

800 **Table 3. Metabolic states of mitochondria (Chance and**  
 801 **Williams, 1956; Table V).**

State	[O <sub>2</sub> ]	ADP level	Substrate level	Respiration rate	Rate-limiting substance
1	>0	Low	low	slow	ADP
2	>0	high	~0	slow	substrate
3	>0	high	high	fast	respiratory chain
4	>0	Low	high	slow	ADP
5	0	high	high	0	oxygen

803  
 804 **State 3** is the state stimulated by addition of fuel substrates while the ADP concentration  
 805 is still high (**Table 3**) and supports coupled energy transformation through oxidative  
 806 phosphorylation. ‘High ADP’ is a concentration of ADP specifically selected to allow the  
 807 measurement of State 3 to State 4 transitions of isolated mitochondria in a closed respirometric  
 808 chamber. Repeated ADP titration re-establishes State 3 at ‘high ADP’. Starting at O<sub>2</sub>  
 809 concentrations near air-saturation (ca. 200 μM O<sub>2</sub> at sea level and 37 °C), the total ADP  
 810 concentration added must be low enough (typically 100 to 300 μM) to allow phosphorylation  
 811 to ATP at a coupled O<sub>2</sub> flux that does not lead to O<sub>2</sub> depletion during the transition to State 4.  
 812 In contrast, kinetically-saturating ADP concentrations usually are 10-fold higher than ‘high  
 813 ADP’, e.g., 2.5 mM in isolated mitochondria. The abbreviation State 3u is occasionally used in  
 814 bioenergetics, to indicate the state of respiration after titration of an uncoupler, without  
 815 sufficient emphasis on the fundamental difference between OXPHOS-capacity (*well-coupled*  
 816 with an *endogenous* uncoupled component) and ET-capacity (*noncoupled*).

817 **State 4** is a LEAK-state that is obtained only if the mitochondrial preparation is intact  
 818 and well-coupled. Depletion of ADP by phosphorylation to ATP causes a decline of O<sub>2</sub> flux in  
 819 the transition from State 3 to State 4. Under the conditions of State 4, a maximum protonmotive  
 820 force and high ATP/ADP ratio are maintained. The gradual decline of  $Y_{P_{\gg}/O_2}$  towards  
 821 diminishing [ADP] at State 4 must be taken into account for calculation of  $P_{\gg}/O_2$  ratios (Gnaiger  
 822 2001). State 4 respiration,  $L_T$  (**Table 1**), reflects intrinsic proton leak and ATP hydrolysis  
 823 activity. O<sub>2</sub> flux in State 4 is an overestimation of LEAK-respiration if the contaminating ATP  
 824 hydrolysis activity recycles some ATP to ADP,  $J_{P_{\ll}}$ , which stimulates respiration coupled to  
 825 phosphorylation,  $J_{P_{\gg}} > 0$ . This can be tested by inhibition of the phosphorylation-pathway using  
 826 oligomycin, ensuring that  $J_{P_{\gg}} = 0$  (State 4o). Alternatively, sequential ADP titrations re-  
 827 establish State 3, followed by State 3 to State 4 transitions while sufficient O<sub>2</sub> is available.  
 828 Anoxia may be reached, however, before exhaustion of ADP (State 5).

829 **State 5** is the state after exhaustion of O<sub>2</sub> in a closed respirometric chamber. Diffusion of  
 830 O<sub>2</sub> from the surroundings into the aqueous solution may be a confounding factor preventing  
 831 complete anoxia (Gnaiger 2001). Chance and Williams (1955) provide an alternative definition  
 832 of State 5, which gives it the different meaning of ROX versus anoxia: ‘State 5 may be obtained  
 833 by antimycin A treatment or by anaerobiosis’.

834 In **Table 3**, only States 3 and 4 (and ‘State 2’ in the alternative protocol: addition of fuel  
 835 substrates without ADP; not included in the table) are coupling control states, with the  
 836 restriction that O<sub>2</sub> flux in State 3 may be limited kinetically by non-saturating ADP  
 837 concentrations (**Table 1**).

838

### 839 3. Normalization: fluxes and flows

840

#### 841 3.1. Normalization: system or sample

842

843 The term *rate* is not sufficiently defined to be useful for reporting data (**Fig. 6**). The  
 844 inconsistency of the meanings of rate becomes fully apparent when considering Galileo  
 845 Galilei's famous principle, that 'bodies of different weight all fall at the same rate (have a  
 846 constant acceleration)' (Coopersmith 2010).

847 **Flow per system,  $I$ :** In a generalization of electrical terms, flow as an extensive quantity  
 848 ( $I$ ; per system) is distinguished from flux as a size-specific quantity ( $J$ ; per system size) (**Fig.**  
 849 **6**). Electric current is flow,  $I_{el}$  [ $A \equiv C \cdot s^{-1}$ ] per system (extensive quantity). When dividing this  
 850 extensive quantity by system size (cross-sectional area of a 'wire'), a size-specific quantity is  
 851 obtained, which is flux (current density),  $J_{el}$  [ $A \cdot m^{-2} = C \cdot s^{-1} \cdot m^{-2}$ ].

852 **Extensive quantities:** An extensive quantity increases proportionally with system size.  
 853 The magnitude of an extensive quantity is completely additive for non-interacting  
 854 subsystems—such as mass or flow expressed per defined system. The magnitude of these  
 855 quantities depends on the extent or size of the system (Cohen *et al.* 2008).

856 **Size-specific quantities:** 'The adjective *specific* before the name of an extensive quantity  
 857 is often used to mean *divided by mass*' (Cohen *et al.* 2008). In this system-paradigm, mass-  
 858 specific flux is flow divided by mass of the *system* (the total mass of everything within the  
 859 measuring chamber or reactor). A mass-specific quantity is independent of the extent of non-  
 860 interacting homogenous subsystems. Tissue-specific quantities (related to the *sample* in  
 861 contrast to the *system*) are of fundamental interest in the field of comparative mitochondrial  
 862 physiology, where *specific* refers to the *type of the sample* rather than *mass of the system*. The  
 863 term *specific*, therefore, must be clarified; *sample-specific*, *e.g.*, muscle mass-specific  
 864 normalization, is distinguished from *system-specific* quantities (mass or volume; **Fig. 6**).

865

866 **Fig. 6. Different meanings of rate may lead to confusion, if the normalization is not sufficiently specified.** Results are  
 867 frequently expressed as mass-specific flux,  $J_{mX}$ , per mg protein, dry or wet weight (mass). Cell  
 868 volume,  $V_{cell}$ , may be used for normalization (volume-specific flux,  $J_{Vcell}$ ), which must be clearly  
 869 distinguished from flow per cell,  $I_{Ncell}$ , or flux,  $J_V$ , expressed for methodological reasons per  
 870 volume of the measurement system. For details see **Table 4**.

871

872

873

874

875

876

877

878

879

880

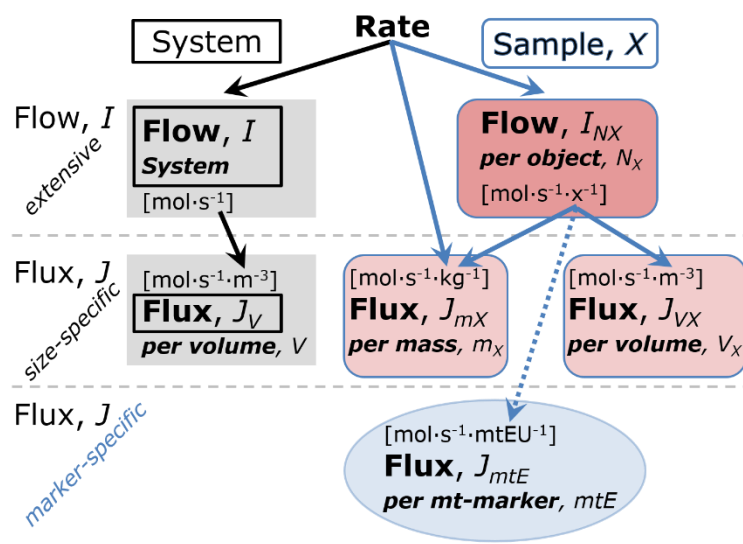
881

882

883

884

885



881

882

883

#### 883 **Box 2: Metabolic fluxes and flows: vectorial and scalar**

884

885

886

887

888

889

889

886 Fluxes are *vectors*, if they have *spatial* geometric direction in addition to magnitude.  
 887 Electric charge per unit time is electric flow or current,  $I_{el} = dQ_{el} \cdot dt^{-1}$  [A]. When expressed per  
 888 unit cross-sectional area,  $A$  [ $m^2$ ], a vector flux is obtained, which is current density or surface-  
 889 density of flow) perpendicular to the direction of flux,  $J_{el} = I_{el} \cdot A^{-1}$  [ $A \cdot m^{-2}$ ] (Cohen *et al.* 2008).  
 For all transformations *flows*,  $I_{tr}$ , are defined as extensive quantities. Vector and scalar *fluxes*

890 are obtained as  $J_{tr} = I_{tr} \cdot A^{-1}$  [ $\text{mol} \cdot \text{s}^{-1} \cdot \text{m}^{-2}$ ] and  $J_{tr} = I_{tr} \cdot V^{-1}$  [ $\text{mol} \cdot \text{s}^{-1} \cdot \text{m}^{-3}$ ], expressing flux as an area-  
 891 specific vector or volume-specific vectorial or scalar quantity, respectively (Gnaiger 1993b).

892 We suggest to define: (1) *vectorial* fluxes, which are translocations as functions of  
 893 *gradients* with direction in geometric space in continuous systems; (2) *vectorial* fluxes, which  
 894 describe translocations in discontinuous systems and are restricted to information on  
 895 *compartmental differences* (**Fig. 2C**, transmembrane proton flux); and (3) *scalar* fluxes, which  
 896 are transformations in a *homogenous* system (**Fig. 2C**, catabolic O<sub>2</sub> flux,  $J_{\text{kO}_2}$ ).

897 Vectorial transmembrane proton fluxes,  $J_{\text{mH}^+\text{pos}}$  and  $J_{\text{mH}^+\text{neg}}$ , are analyzed in a  
 898 heterogenous compartmental system as a quantity with *directional* but not *spatial* information.  
 899 Translocation of protons across the mtIM has a defined direction, either from the negative  
 900 compartment (matrix space; negative, neg–compartment) to the positive compartment (inter-  
 901 membrane space; positive, pos–compartment) or *vice versa* (**Fig. 2C**). The arrows defining the  
 902 direction of the translocation between the two compartments may point upwards or downwards,  
 903 right or left, without any implication that these are actual directions in space. The pos–  
 904 compartment is neither above nor below the neg–compartment in a spatial sense, but can be  
 905 visualized arbitrarily in a figure in the upper position (**Fig. 2C**). In general, the *compartmental*  
 906 *direction* of vectorial translocation from the neg–compartment to the pos–compartment is  
 907 defined by assigning the initial and final state as *ergodynamic compartments*,  $\text{H}^+_{\text{neg}} \rightarrow \text{H}^+_{\text{pos}}$  or  
 908  $0 = -1 \text{H}^+_{\text{neg}} + 1 \text{H}^+_{\text{pos}}$ , related to work (erg = work) that must be performed to lift the proton from  
 909 a lower to a higher electrochemical potential or from the lower to the higher ergodynamic  
 910 compartment (Gnaiger 1993b).

911 In analogy to *vectorial* translocation, the direction of a *scalar* chemical reaction,  $\text{A} \rightarrow \text{B}$   
 912 or  $0 = -1 \text{A} + 1 \text{B}$ , is defined by assigning substrates and products, A and B, as ergodynamic  
 913 compartments. O<sub>2</sub> is defined as a substrate in respiratory O<sub>2</sub> consumption, which together with  
 914 the fuel substrates comprises the substrate compartment of the catabolic reaction. Volume-  
 915 specific scalar O<sub>2</sub> flux is coupled to vectorial translocation, yielding the  $\text{H}^+_{\text{pos}}/\text{O}_2$  ratio (**Fig. 2**).  
 916

917

### 918 3.2. Normalization for system-size: flux per chamber volume

919

920 **System-specific flux,  $J_{V,\text{O}_2}$ :** The experimental system (experimental chamber) is part of  
 921 the measurement apparatus, separated from the environment as an isolated, closed, open,  
 922 isothermal or non-isothermal system (**Table 4**). On another level, we distinguish between (1)  
 923 the *system* with volume  $V$  and mass  $m$  defined by the system boundaries, and (2) the *sample* or  
 924 *objects* with volume  $V_X$  and mass  $m_X$  which are enclosed in the experimental chamber (**Fig. 6**).  
 925 Metabolic O<sub>2</sub> flow per object,  $I_{\text{O}_2/X}$ , increases as the mass of the object is increased. Sample  
 926 mass-specific O<sub>2</sub> flux,  $J_{\text{O}_2/mX}$  should be independent of the mass of the sample studied in the  
 927 instrument chamber, but system volume-specific O<sub>2</sub> flux,  $J_{V,\text{O}_2}$  (per volume of the instrument  
 928 chamber), should increase in direct proportion to the mass of the sample in the chamber.  
 929 Whereas  $J_{V,\text{O}_2}$  depends on mass-concentration of the sample in the chamber, it should be  
 930 independent of the chamber (system) volume at constant sample mass. There are practical  
 931 limitations to increase the mass-concentration of the sample in the chamber, when one is  
 932 concerned about crowding effects and instrumental time resolution.

933 When the reactor volume does not change during the reaction, which is typical for liquid  
 934 phase reactions, the volume-specific *flux of a chemical reaction*  $r$  is the time derivative of the  
 935 advancement of the reaction per unit volume,  $J_{V,rB} = d_r \zeta_B / dt \cdot V^{-1}$  [ $(\text{mol} \cdot \text{s}^{-1}) \cdot \text{L}^{-1}$ ]. The *rate of*  
 936 *concentration change* is  $dc_B / dt$  [ $(\text{mol} \cdot \text{L}^{-1}) \cdot \text{s}^{-1}$ ], where concentration is  $c_B = n_B / V$ . There is a  
 937 difference between (1)  $J_{V,r\text{O}_2}$  [ $\text{mol} \cdot \text{s}^{-1} \cdot \text{L}^{-1}$ ] and (2) rate of concentration change [ $\text{mol} \cdot \text{L}^{-1} \cdot \text{s}^{-1}$ ].  
 938 These merge to a single expression only in closed systems. In open systems, external fluxes  
 939 (such as O<sub>2</sub> supply) are distinguished from internal transformations (catabolic flux, O<sub>2</sub>  
 940 consumption). In a closed system, external flows of all substances are zero and O<sub>2</sub> consumption

941 (internal flow of catabolic reactions  $k$ ),  $I_{kO_2}$  [ $\text{pmol}\cdot\text{s}^{-1}$ ], causes a decline of the amount of  $O_2$  in  
 942 the system,  $n_{O_2}$  [ $\text{nmol}$ ]. Normalization of these quantities for the volume of the system,  $V$  [ $\text{L} \equiv$   
 943  $\text{dm}^3$ ], yields volume-specific  $O_2$  flux,  $J_{V,kO_2} = I_{kO_2}/V$  [ $\text{nmol}\cdot\text{s}^{-1}\cdot\text{L}^{-1}$ ], and  $O_2$  concentration,  $[O_2]$   
 944 or  $c_{O_2} = n_{O_2}/V$  [ $\mu\text{mol}\cdot\text{L}^{-1} = \mu\text{M} = \text{nmol}\cdot\text{mL}^{-1}$ ]. Instrumental background  $O_2$  flux is due to external  
 945 flux into a non-ideal closed respirometer; then total volume-specific flux has to be corrected for  
 946 instrumental background  $O_2$  flux— $O_2$  diffusion into or out of the instrumental chamber.  $J_{V,kO_2}$   
 947 is relevant mainly for methodological reasons and should be compared with the accuracy of  
 948 instrumental resolution of background-corrected flux, *e.g.*,  $\pm 1 \text{ nmol}\cdot\text{s}^{-1}\cdot\text{L}^{-1}$  (Gnaiger 2001).  
 949 ‘Metabolic’ or catabolic indicates  $O_2$  flux,  $J_{kO_2}$ , corrected for: (1) instrumental background  $O_2$   
 950 flux; (2) chemical background  $O_2$  flux due to autoxidation of chemical components added to  
 951 the incubation medium; and (3)  $R_{ox}$  for  $O_2$ -consuming side reactions unrelated to the catabolic  
 952 pathway  $k$ .

953

### 954 3.3. Normalization: per sample

955

956 The challenges of measuring mitochondrial respiratory flux are matched by those of  
 957 normalization. Application of common and defined units is required for direct transfer of  
 958 reported results into a database. The second [s] is the *SI* unit for the base quantity *time*. It is also  
 959 the standard time-unit used in solution chemical kinetics. A rate may be considered as the  
 960 numerator and normalization as the complementary denominator, which are tightly linked in  
 961 reporting the measurements in a format commensurate with the requirements of a database.  
 962 Normalization (Table 4) is guided by physicochemical principles, methodological  
 963 considerations, and conceptual strategies (Fig. 7).

964 **Sample concentration,  $C_{mX}$ :** Normalization for sample concentration is required to  
 965 report respiratory data. Considering a tissue or cells as the sample,  $X$ , the sample mass is  $m_X$   
 966 [ $\text{mg}$ ], which is frequently measured as wet or dry weight,  $W_w$  or  $W_d$  [ $\text{mg}$ ], respectively, or as  
 967 amount of tissue or cell protein,  $m_{\text{Protein}}$ . In the case of permeabilized tissues, cells, and  
 968 homogenates, the sample concentration,  $C_{mX} = m_X/V$  [ $\text{g}\cdot\text{L}^{-1} = \text{mg}\cdot\text{mL}^{-1}$ ], is the mass of the  
 969 subsample of tissue that is transferred into the instrument chamber.

970 **Mass-specific flux,  $J_{O_2/mX}$ :** Mass-specific flux is obtained by expressing respiration per  
 971 mass of sample,  $m_X$  [ $\text{mg}$ ].  $X$  is the type of sample—isolated mitochondria, tissue homogenate,  
 972 permeabilized fibres or cells. Volume-specific flux is divided by mass concentration of  $X$ ,  $J_{O_2/mX}$   
 973  $= J_{V,O_2}/C_{mX}$ ; or flow per cell is divided by mass per cell,  $J_{O_2/m\text{cell}} = I_{O_2/\text{cell}}/M_{\text{cell}}$ . If mass-specific  
 974  $O_2$  flux is constant and independent of sample size (expressed as mass), then there is no  
 975 interaction between the subsystems. A 1.5 mg and a 3.0 mg muscle sample respire at identical  
 976 mass-specific flux. Mass-specific  $O_2$  flux, however, may change with the mass of a tissue  
 977 sample, cells or isolated mitochondria in the measuring chamber, in which the nature of the  
 978 interaction becomes an issue. Therefore, cell density must be optimized, particularly in  
 979 experiments carried out in wells, considering the confluency of the cell monolayer or clumps  
 980 of cells (Salabei *et al.* 2014).

981 **Number concentration,  $C_{NX}$ :**  $C_{NX}$  is the experimental *number concentration* of sample  
 982  $X$ . In the case of cells or animals, *e.g.*, nematodes,  $C_{NX} = N_X/V$  [ $\text{x}\cdot\text{L}^{-1}$ ], where  $N_X$  is the number  
 983 of cells or organisms in the chamber (Table 4).

984 **Flow per object,  $I_{O_2/X}$ :** A special case of normalization is encountered in respiratory  
 985 studies with permeabilized (or intact) cells. If respiration is expressed per cell, the  $O_2$  flow per  
 986 measurement system is replaced by the  $O_2$  flow per cell,  $I_{O_2/\text{cell}}$  (Table 4).  $O_2$  flow can be  
 987 calculated from volume-specific  $O_2$  flux,  $J_{V,O_2}$  [ $\text{nmol}\cdot\text{s}^{-1}\cdot\text{L}^{-1}$ ] (per  $V$  of the measurement chamber  
 988 [ $\text{L}$ ]), divided by the number concentration of cells,  $C_{N\text{cell}} = N_{\text{cell}}/V$  [ $\text{cell}\cdot\text{L}^{-1}$ ], where  $N_{\text{cell}}$  is the  
 989 number of cells in the chamber. The total cell count is the sum of viable and dead cells,  $N_{\text{cell}} =$   
 990  $N_{\text{vce}} + N_{\text{dce}}$  (Table 5). The cell viability index,  $\text{CVI} = N_{\text{vce}}/N_{\text{cell}}$ , is the ratio of viable cells ( $N_{\text{vce}}$ ;  
 991 before experimental permeabilization) per total cell count. After experimental permeabilization,



992 all cells are permeabilized,  $N_{pce} = N_{cell}$ . The cell viability index can be used to normalize  
 993 respiration for the number of cells that have been viable before experimental permeabilization,  
 994  $I_{O_2/vce} = I_{O_2/cell}/CVI$ , considering that mitochondrial respiratory dysfunction in dead cells should  
 995 be eliminated as a confounding factor.

996  
 997  
 998

**Table 4. Sample concentrations and normalization of flux.**

Expression	Symbol	Definition	Unit	Notes
<b>Sample</b>				
identity of sample	$X$	object: cell, tissue, animal, patient		
number of sample entities $X$	$N_X$	number of objects	x	
mass of sample $X$	$m_X$		kg	1
mass of object $X$	$M_X$	$M_X = m_X \cdot N_X^{-1}$	$\text{kg} \cdot \text{x}^{-1}$	1
<b>Mitochondria</b>				
mitochondria	mt	$X = \text{mt}$		
amount of mt-elements	$mtE$	quantity of mt-marker	mtEU	
<b>Concentrations</b>				
object number concentration	$C_{NX}$	$C_{NX} = N_X \cdot V^{-1}$	$\text{x} \cdot \text{m}^{-3}$	2
sample mass concentration	$C_{mX}$	$C_{mX} = m_X \cdot V^{-1}$	$\text{kg} \cdot \text{m}^{-3}$	
mitochondrial concentration	$C_{mtE}$	$C_{mtE} = mtE \cdot V^{-1}$	$\text{mtEU} \cdot \text{m}^{-3}$	3
specific mitochondrial density	$D_{mtE}$	$D_{mtE} = mtE \cdot m_X^{-1}$	$\text{mtEU} \cdot \text{kg}^{-1}$	4
mitochondrial content, $mtE$ per object $X$	$mtE_X$	$mtE_X = mtE \cdot N_X^{-1}$	$\text{mtEU} \cdot \text{x}^{-1}$	5
<b>O<sub>2</sub> flow and flux</b>				
flow, system	$I_{O_2}$	internal flow	$\text{mol} \cdot \text{s}^{-1}$	6
volume-specific flux	$J_{V,O_2}$	$J_{V,O_2} = I_{O_2} \cdot V^{-1}$	$\text{mol} \cdot \text{s}^{-1} \cdot \text{m}^{-3}$	7
flow per object $X$	$I_{O_2/X}$	$I_{O_2/X} = J_{V,O_2} \cdot C_{NX}^{-1}$	$\text{mol} \cdot \text{s}^{-1} \cdot \text{x}^{-1}$	8
mass-specific flux	$J_{O_2/mX}$	$J_{O_2/mX} = J_{V,O_2} \cdot C_{mX}^{-1}$	$\text{mol} \cdot \text{s}^{-1} \cdot \text{kg}^{-1}$	9
mitochondria-specific flux	$J_{O_2/mtE}$	$J_{O_2/mtE} = J_{V,O_2} \cdot C_{mtE}^{-1}$	$\text{mol} \cdot \text{s}^{-1} \cdot \text{mtEU}^{-1}$	10

- 999 1 The SI prefix k is used for the SI base unit of mass (kg = 1,000 g). In praxis, various SI prefixes are  
 1000 used for convenience, to make numbers easily readable, e.g., 1 mg tissue, cell or mitochondrial mass  
 1001 instead of 0.000001 kg.
- 1002 2 In case sample  $X = \text{cells}$ , the object number concentration is  $C_{N_{cell}} = N_{cell} \cdot V^{-1}$ , and volume may be  
 1003 expressed in [ $\text{dm}^3 \equiv \text{L}$ ] or [ $\text{cm}^3 = \text{mL}$ ]. See **Table 5** for different object types.
- 1004 3 mt-concentration is an experimental variable, dependent on sample concentration: (1)  $C_{mtE} = mtE \cdot V^{-1}$ ;  
 1005 (2)  $C_{mtE} = mtE_X \cdot C_{NX}$ ; (3)  $C_{mtE} = C_{mX} \cdot D_{mtE}$ .
- 1006 4 If the amount of mitochondria,  $mtE$ , is expressed as mitochondrial mass, then  $D_{mtE}$  is the mass  
 1007 fraction of mitochondria in the sample. If  $mtE$  is expressed as mitochondrial volume,  $V_{mt}$ , and the  
 1008 mass of sample,  $m_X$ , is replaced by volume of sample,  $V_X$ , then  $D_{mtE}$  is the volume fraction of  
 1009 mitochondria in the sample.
- 1010 5  $mtE_X = mtE \cdot N_X^{-1} = C_{mtE} \cdot C_{NX}^{-1}$ .
- 1011 6 O<sub>2</sub> can be replaced by other chemicals B to study different reactions, e.g., ATP, H<sub>2</sub>O<sub>2</sub>, or  
 1012 compartmental translocations, e.g., Ca<sup>2+</sup>.
- 1013 7  $I_{O_2}$  and  $V$  are defined per instrument chamber as a system of constant volume (and constant  
 1014 temperature), which may be closed or open.  $I_{O_2}$  is abbreviated for  $I_{r,O_2}$ , i.e., the metabolic or internal  
 1015 O<sub>2</sub> flow of the chemical reaction  $r$  in which O<sub>2</sub> is consumed, hence the negative stoichiometric  
 1016 number,  $\nu_{O_2} = -1$ .  $I_{r,O_2} = d_r n_{O_2} / dt \cdot \nu_{O_2}^{-1}$ . If  $r$  includes all chemical reactions in which O<sub>2</sub> participates, then  
 1017  $d_r n_{O_2} = dn_{O_2} - d_e n_{O_2}$ , where  $dn_{O_2}$  is the change in the amount of O<sub>2</sub> in the instrument chamber and  $d_e n_{O_2}$   
 1018 is the amount of O<sub>2</sub> added externally to the system. At steady state, by definition  $dn_{O_2} = 0$ , hence  $d_r n_{O_2}$   
 1019  $= -d_e n_{O_2}$ .



- 1020 8  $J_{V,O_2}$  is an experimental variable, expressed per volume of the instrument chamber.  
 1021 9  $I_{O_2/X}$  is a physiological variable, depending on the size of entity  $X$ .  
 1022 10 There are many ways to normalize for a mitochondrial marker, that are used in different experimental  
 1023 approaches: (1)  $J_{O_2/mtE} = J_{V,O_2} \cdot C_{mtE}^{-1}$ ; (2)  $J_{O_2/mtE} = J_{V,O_2} \cdot C_{mX}^{-1} \cdot D_{mtE}^{-1} = J_{O_2/mX} \cdot D_{mtE}^{-1}$ ; (3)  $J_{O_2/mtE} =$   
 1024  $J_{V,O_2} \cdot C_{NX}^{-1} \cdot mtE_X^{-1} = I_{O_2/X} \cdot mtE_X^{-1}$ ; (4)  $J_{O_2/mtE} = I_{O_2} \cdot mtE^{-1}$ . The mt-elemental unit [mtEU] varies between  
 1025 different mt-markers.  
 1026  
 1027

**Table 5. Sample types, X, abbreviations, and quantification.**

Identity of sample	$X$	$N_X$	Mass <sup>a</sup>	Volume	mt-Marker
mitochondrial preparation	mt-prep	[x]	[kg]	[m <sup>3</sup> ]	[mtEU]
isolated mitochondria	imt		$m_{mt}$	$V_{mt}$	$mtE$
tissue homogenate	thom		$m_{thom}$		$mtE_{thom}$
permeabilized tissue	pti		$m_{pti}$		$mtE_{pti}$
permeabilized fibre	pfi		$m_{pfi}$		$mtE_{pfi}$
permeabilized cell	pce	$N_{pce}$	$M_{pce}$	$V_{pce}$	$mtE_{pce}$
cells <sup>b</sup>	cell	$N_{cell}$	$M_{cell}$	$V_{cell}$	$mtE_{cell}$
intact cell, viable cell	vce	$N_{vce}$	$M_{vce}$	$V_{vce}$	
dead cell	dce	$N_{dce}$	$M_{dce}$	$V_{dce}$	
organism	org	$N_{org}$	$M_{org}$	$V_{org}$	

<sup>a</sup> Instead of mass, the wet weight or dry weight is frequently stated,  $W_w$  or  $W_d$ .  
 $m_X$  is mass of the sample [kg],  $M_X$  is mass of the object [kg·x<sup>-1</sup>].

<sup>b</sup> Total cell count,  $N_{cell} = N_{vce} + N_{dce}$

1028  
 1029  
 1030  
 1031  
 1032 Cellular O<sub>2</sub> flow can be compared between cells of identical size. To take into account  
 1033 changes and differences in cell size, normalization is required to obtain cell size-specific or  
 1034 mitochondrial marker-specific O<sub>2</sub> flux (Renner *et al.* 2003).

1035 The complexity changes when the sample is a whole organism studied as an experimental  
 1036 model. The scaling law in respiratory physiology reveals a strong interaction of O<sub>2</sub> flow and  
 1037 individual body mass of an organism, since *basal* metabolic rate (flow) does not increase  
 1038 linearly with body mass, whereas *maximum* mass-specific O<sub>2</sub> flux,  $\dot{V}_{O_2max}$  or  $\dot{V}_{O_2peak}$ , is  
 1039 approximately constant across a large range of individual body mass (Weibel and Hoppeler  
 1040 2005), with individuals, breeds, and species deviating substantially from this relationship.  
 1041  $\dot{V}_{O_2peak}$  of human endurance athletes is 60 to 80 mL O<sub>2</sub>·min<sup>-1</sup>·kg<sup>-1</sup> body mass, converted to  
 1042  $J_{O_2peak/M}$  of 45 to 60 nmol·s<sup>-1</sup>·g<sup>-1</sup> (Gnaiger 2014; **Table 6**).

### 1044 3.4. Normalization for mitochondrial content

1045  
 1046 Tissues can contain multiple cell populations that may have distinct mitochondrial  
 1047 subtypes. Mitochondria undergo dynamic fission and fusion cycles, and can exist in multiple  
 1048 stages and sizes that may be altered by a range of factors. The isolation of mitochondria (often  
 1049 achieved through differential centrifugation) can therefore yield a subsample of the  
 1050 mitochondrial types present in a tissue, depending on the isolation protocols utilized (*e.g.*,  
 1051 centrifugation speed). This possible bias should be taken into account when planning  
 1052 experiments using isolated mitochondria. Different sizes of mitochondria are enriched at  
 1053 specific centrifugation speeds, which can be used strategically for isolation of mitochondrial  
 1054 subpopulations.

<b>Flow, Performance</b>	=	<b>Element function</b>	x	<b>Element density</b>	x	<b>Size of object</b>
$\frac{\text{mol}\cdot\text{s}^{-1}}{x}$	=	$\frac{\text{mol}\cdot\text{s}^{-1}}{x_{mtE}}$	·	$\frac{x_{mtE}}{\text{kg}}$	·	$\frac{\text{kg}}{x}$

A

<b>Flow</b>	=	<b>mt-specific flux</b>	x	<b>mt-structure, functional elements</b>
$I_{O_2/X}$	=	$J_{O_2/mtE}$	·	$mtE_X$
				$\frac{mtE_X}{M_X} \cdot M_X$

$I_{O_2/X}$	=	$J_{O_2/mtE}$	·	$D_{mtE}$	·	$M_X$
$\frac{I_{O_2/X}}{M_X}$	=	$\frac{I_{O_2/X}}{mtE_X}$	·	$\frac{mtE_X}{M_X}$		

B

$I_{O_2/X}$	=	$J_{O_2/MX}$	·	$M_X$
<b>Flow</b>	=	<b>Object mass-specific flux</b>	x	<b>Mass of object</b>

**Fig. 7. Structure-function analysis of performance of an organism, organ or tissue, or a cell (sample entity, X). O<sub>2</sub> flow,  $I_{O_2/X}$ , is the product of performance per functional element (element function, mitochondria-specific flux), element density (mitochondrial density,  $D_{mtE}$ ), and size of entity X (mass,  $M_X$ ). (A) Structured analysis: performance is the product of mitochondrial function (mt-specific flux) and structure (functional elements;  $D_{mtE}$  times mass of X). (B) Unstructured analysis: performance is the product of entity mass-specific flux,  $J_{O_2/MX} = I_{O_2/X}/M_X = I_{O_2}/m_X$  [mol·s<sup>-1</sup>·kg<sup>-1</sup>] and size of entity, expressed as mass of X;  $M_X = m_X \cdot N_X^{-1}$  [kg·x<sup>-1</sup>]. See Table 4 for further explanation of quantities and units. Modified from Gnaiger (2014).**

Part of the mitochondrial content of a tissue is lost during preparation of isolated mitochondria. The fraction of isolated mitochondria obtained from a tissue sample is expressed as mitochondrial recovery. At a high mitochondrial recovery the fraction of isolated mitochondria is more representative of the total mitochondrial population than in preparations characterized by low recovery. Determination of the mitochondrial recovery and yield is based on measurement of the concentration of a mitochondrial marker in the stock of isolated mitochondria,  $C_{mtE,stock}$ , and crude tissue homogenate,  $C_{mtE,thom}$ , which simultaneously provides information on the specific mitochondrial density in the sample,  $D_{mtE}$  (Table 4).

Normalization is a problematic subject; it is essential to consider the question of the study. If the study aims at comparing tissue performance—such as the effects of a treatment on a specific tissue, then normalization for tissue mass or protein content is appropriate. However, if the aim is to find differences on mitochondrial function independent of mitochondrial density (Table 4), then normalization to a mitochondrial marker is imperative (Fig. 7). One cannot assume that quantitative changes in various markers—such as mitochondrial proteins—necessarily occur in parallel with one another. It should be established that the marker chosen is not selectively altered by the performed treatment. In conclusion, the normalization must reflect the question under investigation to reach a satisfying answer. On the other hand, the goal of comparing results across projects and institutions requires standardization on normalization for entry into a databank.

**Mitochondrial concentration,  $C_{mtE}$ , and mitochondrial markers:** Mitochondrial organelles comprise a dynamic cellular reticulum in various states of fusion and fission. Hence, the definition of an "amount" of mitochondria is often misconceived: mitochondria cannot be

1088 counted reliably as a number of occurring elements. Therefore, quantification of the "amount"  
 1089 of mitochondria depends on the measurement of chosen mitochondrial markers. 'Mitochondria  
 1090 are the structural and functional elemental units of cell respiration' (Gnaiger 2014). The  
 1091 quantity of a mitochondrial marker can reflect the amount of *mitochondrial elements*,  $mtE$ ,  
 1092 expressed in various mitochondrial elemental units [mtEU] specific for each measured mt-  
 1093 marker (**Table 4**). However, since mitochondrial quality may change in response to stimuli—  
 1094 particularly in mitochondrial dysfunction and after exercise training (Pesta *et al.* 2011; Campos  
 1095 *et al.* 2017)—some markers can vary while others are unchanged: (1) Mitochondrial volume  
 1096 and membrane area are structural markers, whereas mitochondrial protein mass is frequently  
 1097 used as a marker for isolated mitochondria. (2) Molecular and enzymatic mitochondrial markers  
 1098 (amounts or activities) can be selected as matrix markers, *e.g.*, citrate synthase activity, mtDNA;  
 1099 mtIM-markers, *e.g.*, cytochrome *c* oxidase activity,  $aa_3$  content, cardiolipin, or mtOM-markers,  
 1100 *e.g.*, TOM20. (3) Extending the measurement of mitochondrial marker enzyme activity to  
 1101 mitochondrial pathway capacity, ET- or OXPHOS-capacity can be considered as an integrative  
 1102 functional mitochondrial marker.

1103 Depending on the type of mitochondrial marker, the mitochondrial elements,  $mtE$ , are  
 1104 expressed in marker-specific units. Mitochondrial concentration in the measurement chamber  
 1105 and the tissue of origin are quantified as (1) a quantity for normalization in functional analyses,  
 1106  $C_{mtE}$ , and (2) a physiological output that is the result of mitochondrial biogenesis and  
 1107 degradation,  $D_{mtE}$ , respectively (**Table 4**). It is recommended, therefore, to distinguish  
 1108 *experimental mitochondrial concentration*,  $C_{mtE} = mtE/V$  and *physiological mitochondrial*  
 1109 *density*,  $D_{mtE} = mtE/m_X$ . Then mitochondrial density is the amount of mitochondrial elements  
 1110 per mass of tissue, which is a biological variable (**Fig. 7**). The experimental variable is  
 1111 mitochondrial density multiplied by sample mass concentration in the measuring chamber,  $C_{mtE}$   
 1112  $= D_{mtE} \cdot C_{mX}$ , or mitochondrial content multiplied by sample number concentration,  $C_{mtE} =$   
 1113  $mtE_X \cdot C_{NX}$  (**Table 4**).

1114 **Mitochondria-specific flux,  $J_{O_2/mtE}$** : Volume-specific metabolic  $O_2$  flux depends on: (1)  
 1115 the sample concentration in the volume of the instrument chamber,  $C_{mX}$ , or  $C_{NX}$ ; (2) the  
 1116 mitochondrial density in the sample,  $D_{mtE} = mtE/m_X$  or  $mtE_X = mtE/N_X$ ; and (3) the specific  
 1117 mitochondrial activity or performance per elemental mitochondrial unit,  $J_{O_2/mtE} = J_{V,O_2}/C_{mtE}$   
 1118 [ $mol \cdot s^{-1} \cdot mtEU^{-1}$ ] (**Table 4**). Obviously, the numerical results for  $J_{O_2/mtE}$  vary with the type of  
 1119 mitochondrial marker chosen for measurement of  $mtE$  and  $C_{mtE} = mtE/V$  [ $mtEU \cdot m^{-3}$ ].

1120

### 1121 3.5. Evaluation of mitochondrial markers

1122

1123 Different methods are implicated in the quantification of mitochondrial markers and have  
 1124 different strengths. Some problems are common for all mitochondrial markers,  $mtE$ : (1)  
 1125 Accuracy of measurement is crucial, since even a highly accurate and reproducible  
 1126 measurement of  $O_2$  flux results in an inaccurate and noisy expression if normalized by a biased  
 1127 and noisy measurement of a mitochondrial marker. This problem is acute in mitochondrial  
 1128 respiration because the denominators used (the mitochondrial markers) are often small moieties  
 1129 of which accurate and precise determination is difficult. This problem can be avoided when  $O_2$   
 1130 fluxes measured in substrate-uncoupler-inhibitor titration protocols are normalized for flux in  
 1131 a defined respiratory reference state, which is used as an *internal* marker and yields flux control  
 1132 ratios, *FCRs*. *FCRs* are independent of *externally* measured markers and, therefore, are  
 1133 statistically robust, considering the limitations of ratios in general (Jasienski and Bazzaz 1999).  
 1134 *FCRs* indicate qualitative changes of mitochondrial respiratory control, with highest  
 1135 quantitative resolution, separating the effect of mitochondrial density or concentration on  $J_{O_2/mX}$   
 1136 and  $I_{O_2/X}$  from that of function per elemental mitochondrial marker,  $J_{O_2/mtE}$  (Pesta *et al.* 2011;  
 1137 Gnaiger 2014). (2) If mitochondrial quality does not change and only the amount of  
 1138 mitochondria varies as a determinant of mass-specific flux, any marker is equally qualified in

1139 principle; then in practice selection of the optimum marker depends only on the accuracy and  
1140 precision of measurement of the mitochondrial marker. (3) If mitochondrial flux control ratios  
1141 change, then there may not be any best mitochondrial marker. In general, measurement of  
1142 multiple mitochondrial markers enables a comparison and evaluation of normalization for a  
1143 variety of mitochondrial markers. Particularly during postnatal development, the activity of  
1144 marker enzymes—such as cytochrome *c* oxidase and citrate synthase—follows different time  
1145 courses (Drahota *et al.* 2004). Evaluation of mitochondrial markers in healthy controls is  
1146 insufficient for providing guidelines for application in the diagnosis of pathological states and  
1147 specific treatments.

1148 In line with the concept of the respiratory control ratio (Chance and Williams 1955a), the  
1149 most readily used normalization is that of flux control ratios and flux control factors (Gnaiger  
1150 2014). Selection of the state of maximum flux in a protocol as the reference state has the  
1151 advantages of: (1) internal normalization; (2) statistical linearization of the response in the range  
1152 of 0 to 1; and (3) consideration of maximum flux for integrating a large number of elemental  
1153 steps in the OXPHOS- or ET-pathways. This reduces the risk of selecting a functional marker  
1154 that is specifically altered by the treatment or pathology, yet increases the chance that the highly  
1155 integrative pathway is disproportionately affected, *e.g.*, the OXPHOS- rather than ET-pathway  
1156 in case of an enzymatic defect in the phosphorylation-pathway. In this case, additional  
1157 information can be obtained by reporting flux control ratios based on a reference state which  
1158 indicates stable tissue-mass specific flux. Stereological determination of mitochondrial content  
1159 via two-dimensional transmission electron microscopy can have limitations due to the dynamics  
1160 of mitochondrial size (Meinild Lundby *et al.* 2017). Accurate determination of three-  
1161 dimensional volume by two-dimensional microscopy can be both time consuming and  
1162 statistically challenging (Larsen *et al.* 2012).

1163 The validity of using mitochondrial marker enzymes (citrate synthase activity, Complex  
1164 I–IV amount or activity) for normalization of flux is limited in part by the same factors that  
1165 apply to flux control ratios. Strong correlations between various mitochondrial markers and  
1166 citrate synthase activity (Reichmann *et al.* 1985; Boushel *et al.* 2007; Mogensen *et al.* 2007)  
1167 are expected in a specific tissue of healthy subjects and in disease states not specifically  
1168 targeting citrate synthase. Citrate synthase activity is acutely modifiable by exercise  
1169 (Tonkonogi *et al.* 1997; Leek *et al.* 2001). Evaluation of mitochondrial markers related to a  
1170 selected age and sex cohort cannot be extrapolated to provide recommendations for  
1171 normalization in respirometric diagnosis of disease, in different states of development and  
1172 ageing, different cell types, tissues, and species. mtDNA normalized to nDNA via qPCR is  
1173 correlated to functional mitochondrial markers including OXPHOS- and ET-capacity in some  
1174 cases (Puntschart *et al.* 1995; Wang *et al.* 1999; Menshikova *et al.* 2006; Boushel *et al.* 2007),  
1175 but lack of such correlations have been reported (Menshikova *et al.* 2005; Schultz and Wiesner  
1176 2000; Pesta *et al.* 2011). Several studies indicate a strong correlation between cardiolipin  
1177 content and increase in mitochondrial function with exercise (Menshikova *et al.* 2005;  
1178 Menshikova *et al.* 2007; Larsen *et al.* 2012; Faber *et al.* 2014), but it has not been evaluated as  
1179 a general mitochondrial biomarker in disease.

1180

### 1181 3.6. Conversion: units

1182

1183 Many different units have been used to report the O<sub>2</sub> consumption rate, OCR (**Table 6**).  
1184 *SI* base units provide the common reference to introduce the theoretical principles (**Fig. 6**), and  
1185 are used with appropriately chosen *SI* prefixes to express numerical data in the most practical  
1186 format, with an effort towards unification within specific areas of application (**Table 7**).  
1187 Reporting data in *SI* units—including the mole [mol], coulomb [C], joule [J], and second [s]—  
1188 should be encouraged, particularly by journals which propose the use of *SI* units.

1189

1190  
1191  
1192  
1193**Table 6. Conversion of various units used in respirometry and ergometry.**  $e^-$  is the number of electrons or reducing equivalents.  $z_B$  is the charge number of entity B.

1 Unit	x	Multiplication factor	SI-unit	Note
ng.atom O $\cdot$ s $^{-1}$	(2 $e^-$ )	0.5	nmol O $_2$ $\cdot$ s $^{-1}$	
ng.atom O $\cdot$ min $^{-1}$	(2 $e^-$ )	8.33	pmol O $_2$ $\cdot$ s $^{-1}$	
natom O $\cdot$ min $^{-1}$	(2 $e^-$ )	8.33	pmol O $_2$ $\cdot$ s $^{-1}$	
nmol O $_2$ $\cdot$ min $^{-1}$	(4 $e^-$ )	16.67	pmol O $_2$ $\cdot$ s $^{-1}$	
nmol O $_2$ $\cdot$ h $^{-1}$	(4 $e^-$ )	0.2778	pmol O $_2$ $\cdot$ s $^{-1}$	
mL O $_2$ $\cdot$ min $^{-1}$ at STPD <sup>a</sup>		0.744	$\mu$ mol O $_2$ $\cdot$ s $^{-1}$	1
W = J/s at -470 kJ/mol O $_2$		-2.128	$\mu$ mol O $_2$ $\cdot$ s $^{-1}$	
mA = mC $\cdot$ s $^{-1}$	( $z_{H^+} = 1$ )	10.36	nmol H $^+$ $\cdot$ s $^{-1}$	2
mA = mC $\cdot$ s $^{-1}$	( $z_{O_2} = 4$ )	2.59	nmol O $_2$ $\cdot$ s $^{-1}$	2
nmol H $^+$ $\cdot$ s $^{-1}$	( $z_{H^+} = 1$ )	0.09649	mA	3
nmol O $_2$ $\cdot$ s $^{-1}$	( $z_{O_2} = 4$ )	0.38594	mA	3

1194  
1195  
1196  
1197  
1198  
1199  
1200  
1201

- 1 At standard temperature and pressure dry (STPD: 0 °C = 273.15 K and 1 atm = 101.325 kPa = 760 mmHg), the molar volume of an ideal gas,  $V_m$ , and  $V_{m,O_2}$  is 22.414 and 22.392 L $\cdot$ mol $^{-1}$ , respectively. Rounded to three decimal places, both values yield the conversion factor of 0.744. For comparison at NTPD (20 °C),  $V_{m,O_2}$  is 24.038 L $\cdot$ mol $^{-1}$ . Note that the *SI* standard pressure is 100 kPa.
- 2 The multiplication factor is  $10^6/(z_B \cdot F)$ .
- 3 The multiplication factor is  $z_B \cdot F/10^6$ .

1202  
1203  
1204  
1205  
1206  
1207  
1208  
1209  
1210  
1211

Although volume is expressed as m $^3$  using the *SI* base unit, the litre [dm $^3$ ] is a conventional unit of volume for concentration and is used for most solution chemical kinetics. If one multiplies  $I_{O_2/cell}$  by  $C_{Ncell}$ , then the result will not only be the amount of O $_2$  [mol] consumed per time [s $^{-1}$ ] in one litre [L $^{-1}$ ], but also the change in O $_2$  concentration per second (for any volume of an ideally closed system). This is ideal for kinetic modeling as it blends with chemical rate equations where concentrations are typically expressed in mol $\cdot$ L $^{-1}$  (Wagner *et al.* 2011). In studies of multinuclear cells—such as differentiated skeletal muscle cells—it is easy to determine the number of nuclei but not the total number of cells. A generalized concept, therefore, is obtained by substituting cells by nuclei as the sample entity. This does not hold, however, for enucleated platelets.

1212  
1213  
1214  
1215  
1216  
1217  
1218  
1219  
1220  
1221  
1222  
1223  
1224  
1225  
1226

For studies of cells, we recommend that respiration be expressed, as far as possible, as: (1) O $_2$  flux normalized for a mitochondrial marker, for separation of the effects of mitochondrial quality and content on cell respiration (this includes *FCRs* as a normalization for a functional mitochondrial marker); (2) O $_2$  flux in units of cell volume or mass, for comparison of respiration of cells with different cell size (Renner *et al.* 2003) and with studies on tissue preparations, and (3) O $_2$  flow in units of attomole ( $10^{-18}$  mol) of O $_2$  consumed in a second by each cell [amol $\cdot$ s $^{-1}$  $\cdot$ cell $^{-1}$ ], numerically equivalent to [pmol $\cdot$ s $^{-1}$  $\cdot$ 10 $^{-6}$  cells]. This convention allows information to be easily used when designing experiments in which O $_2$  flow must be considered. For example, to estimate the volume-specific O $_2$  flux in an instrument chamber that would be expected at a particular cell number concentration, one simply needs to multiply the flow per cell by the number of cells per volume of interest. This provides the amount of O $_2$  [mol] consumed per time [s $^{-1}$ ] per unit volume [L $^{-1}$ ]. At an O $_2$  flow of 100 amol $\cdot$ s $^{-1}$  $\cdot$ cell $^{-1}$  and a cell density of 10 $^9$  cells $\cdot$ L $^{-1}$  (10 $^6$  cells $\cdot$ mL $^{-1}$ ), the volume-specific O $_2$  flux is 100 nmol $\cdot$ s $^{-1}$  $\cdot$ L $^{-1}$  (100 pmol $\cdot$ s $^{-1}$  $\cdot$ mL $^{-1}$ ).



1227

**Table 7. Conversion of units with preservation of numerical values.**

Name	Frequently used unit	Equivalent unit	Note
volume-specific flux, $J_{V,O_2}$	$\text{pmol}\cdot\text{s}^{-1}\cdot\text{mL}^{-1}$ $\text{mmol}\cdot\text{s}^{-1}\cdot\text{L}^{-1}$	$\text{nmol}\cdot\text{s}^{-1}\cdot\text{L}^{-1}$ $\text{mol}\cdot\text{s}^{-1}\cdot\text{m}^{-3}$	1
cell-specific flow, $I_{O_2/\text{cell}}$	$\text{pmol}\cdot\text{s}^{-1}\cdot 10^{-6}$ cells	$\text{amol}\cdot\text{s}^{-1}\cdot\text{cell}^{-1}$	2
	$\text{pmol}\cdot\text{s}^{-1}\cdot 10^{-9}$ cells	$\text{zmol}\cdot\text{s}^{-1}\cdot\text{cell}^{-1}$	3
cell number concentration, $C_{Nce}$	$10^6$ cells $\cdot\text{mL}^{-1}$	$10^9$ cells $\cdot\text{L}^{-1}$	
mitochondrial protein concentration, $C_{mtE}$	$0.1$ mg $\cdot\text{mL}^{-1}$	$0.1$ g $\cdot\text{L}^{-1}$	
mass-specific flux, $J_{O_2/m}$	$\text{pmol}\cdot\text{s}^{-1}\cdot\text{mg}^{-1}$	$\text{nmol}\cdot\text{s}^{-1}\cdot\text{g}^{-1}$	4
catabolic power, $P_k$	$\mu\text{W}\cdot 10^{-6}$ cells	$\text{pW}\cdot\text{cell}^{-1}$	1
Volume	1,000 L	$\text{m}^3$ (1,000 kg)	
	L	$\text{dm}^3$ (kg)	
	mL	$\text{cm}^3$ (g)	
	$\mu\text{L}$	$\text{mm}^3$ (mg)	
	fL	$\mu\text{m}^3$ (pg)	5
amount of substance concentration	$\text{M} = \text{mol}\cdot\text{L}^{-1}$	$\text{mol}\cdot\text{dm}^{-3}$	

1228

1229 1 pmol: picomole =  $10^{-12}$  mol1230 2 amol: attomole =  $10^{-18}$  mol1231 3 zmol: zeptomole =  $10^{-21}$  mol

1232

1233 ET-capacity in human cell types including HEK 293, primary HUVEC and fibroblasts  
 1234 ranges from 50 to 180  $\text{amol}\cdot\text{s}^{-1}\cdot\text{cell}^{-1}$ , measured in intact cells in the noncoupled state (see  
 1235 Gnaiger 2014). At 100  $\text{amol}\cdot\text{s}^{-1}\cdot\text{cell}^{-1}$  corrected for *Rox*, the current across the mt-membranes,  
 1236  $I_{H+e}$ , approximates 193  $\text{pA}\cdot\text{cell}^{-1}$  or 0.2 nA per cell. See Rich (2003) for an extension of  
 1237 quantitative bioenergetics from the molecular to the human scale, with a transmembrane proton  
 1238 flux equivalent to 520 A in an adult at a catabolic power of -110 W. Modelling approaches  
 1239 illustrate the link between protonmotive force and currents (Willis *et al.* 2016).

1240 We consider isolated mitochondria as powerhouses and proton pumps as molecular  
 1241 machines to relate experimental results to energy metabolism of the intact cell. The cellular  
 1242  $\text{P}\gg/\text{O}_2$  based on oxidation of glycogen is increased by the glycolytic (fermentative) substrate-  
 1243 level phosphorylation of 3  $\text{P}\gg/\text{Glyc}$  or 0.5 mol  $\text{P}\gg$  for each mol  $\text{O}_2$  consumed in the complete  
 1244 oxidation of a mol glycosyl unit (Glyc). Adding 0.5 to the mitochondrial  $\text{P}\gg/\text{O}_2$  ratio of 5.4  
 1245 yields a bioenergetic cell physiological  $\text{P}\gg/\text{O}_2$  ratio close to 6. Two NADH equivalents are  
 1246 formed during glycolysis and transported from the cytosol into the mitochondrial matrix, either  
 1247 by the malate-aspartate shuttle or by the glycerophosphate shuttle (**Fig. 1**) resulting in different  
 1248 theoretical yields of ATP generated by mitochondria, the energetic cost of which potentially  
 1249 must be taken into account. Considering also substrate-level phosphorylation in the TCA cycle,  
 1250 this high  $\text{P}\gg/\text{O}_2$  ratio not only reflects proton translocation and OXPHOS studied in isolation,  
 1251 but integrates mitochondrial physiology with energy transformation in the living cell (Gnaiger  
 1252 1993a).

1253

1254

1255 **4. Conclusions**

1256

1257 MitoEAGLE can serve as a gateway to better diagnose mitochondrial respiratory defects  
 1258 linked to genetic variation, age-related health risks, sex-specific mitochondrial performance,  
 1259 lifestyle with its effects on degenerative diseases, and thermal and chemical environment. The  
 1260 present recommendations on coupling control states and rates, linked to the concept of the

1261 protonmotive force, are focused on studies with mitochondrial preparations. These will be  
 1262 extended in a series of reports on pathway control of mitochondrial respiration, respiratory  
 1263 states in intact cells, and harmonization of experimental procedures.  
 1264

---

### 1265 **Box 3: Mitochondrial and cell respiration**

1266  
 1267 Mitochondrial and cell respiration is the process of exergonic and exothermic energy  
 1268 transformation in which scalar redox reactions are coupled to vectorial ion translocation across  
 1269 a semipermeable membrane, which separates the small volume of a bacterial cell or  
 1270 mitochondrion from the larger volume of its surroundings. The electrochemical exergy can be  
 1271 partially conserved in the phosphorylation of ADP to ATP or in ion pumping, or dissipated in  
 1272 an electrochemical short-circuit. Respiration is thus clearly distinguished from fermentation as  
 1273 the counterpart of cellular core energy metabolism (**Fig. 1**). Respiration is separated in  
 1274 mitochondrial preparations from the partial contribution of fermentative pathways of the intact  
 1275 cell. Residual O<sub>2</sub> consumption—as measured after inhibition of mitochondrial electron  
 1276 transfer—does not belong to the class of catabolic reactions coupled to the phosphorylation of  
 1277 ADP to ATP and is, therefore, subtracted from total O<sub>2</sub> consumption to obtain baseline-  
 1278 corrected respiration.

1279 Mitochondrial dysfunction is associated with a wide variety of genetic and degenerative  
 1280 diseases. Robust mitochondrial function is supported by physical exercise and caloric balance,  
 1281 and is central for sustained metabolic health throughout life. Therefore, a consistent  
 1282 presentation of mitochondrial physiology will improve our understanding of the etiology of  
 1283 disease and the diagnostic repertoire of mitochondrial medicine, with a focus on protective  
 1284 medicine, lifestyle and healthy aging.  
 1285

---

1286  
 1287 The optimal choice for expressing mitochondrial and cell respiration (**Box 3**) as O<sub>2</sub> flow  
 1288 per biological sample, and normalization for specific tissue-markers (volume, mass, protein)  
 1289 and mitochondrial markers (volume, protein, content, mtDNA, activity of marker enzymes,  
 1290 respiratory reference state) is guided by the scientific question under study. Interpretation of  
 1291 the data depends critically on appropriate normalization.

1292 We recommend for studies with mitochondrial preparations:

- 1293 • Normalization of respiratory rates should be provided as far as possible: (1) biophysical  
 1294 normalization: on a per cell basis as O<sub>2</sub> flow (may not be possible when dealing with  
 1295 tissues); (2) cellular normalization: per g cell or tissue protein, or per cell or tissue mass  
 1296 as mass-specific O<sub>2</sub> flux; and (3) mitochondrial normalization: per mitochondrial marker  
 1297 as mt-specific flux. With information on cell size and the use of multiple normalizations,  
 1298 maximum potential information is available (Renner *et al.* 2003; Wagner *et al.* 2011;  
 1299 Gnaiger 2014). Reporting flow in a respiratory chamber [nmol·s<sup>-1</sup>] is discouraged, since  
 1300 it restricts the analysis to intra-experimental comparison of relative (qualitative)  
 1301 differences.
- 1302 • Catabolic mitochondrial respiration is distinguished from residual oxygen consumption.  
 1303 Fluxes in mitochondrial coupling states should be, as far as possible, corrected for residual  
 1304 oxygen consumption.
- 1305 • In studies of isolated mitochondria, the mitochondrial recovery and yield should be  
 1306 reported. Experimental criteria for evaluation of purity versus integrity should be  
 1307 considered. Mitochondrial markers—such as citrate synthase activity as an enzymatic  
 1308 matrix marker—provide a link to the tissue of origin on the basis of calculating the  
 1309 mitochondrial recovery, *i.e.*, the fraction of mitochondrial marker obtained from a unit  
 1310 mass of tissue. Total mitochondrial protein is frequently applied as a mitochondrial  
 1311 marker, which is restricted to isolated mitochondria.

- 1312 • In studies of permeabilized cells, the viability of the cell culture or cell suspension of  
 1313 origin should be reported. Normalization should be evaluated for total cell count or viable  
 1314 cell count.
- 1315 • Terms and symbols are summarized in **Table 8**. Their use will facilitate transdisciplinary  
 1316 communication and support further developments towards a consistent theory of  
 1317 bioenergetics and mitochondrial physiology.
- 1318 • Technical terms related to and defined with normal words can be used as index terms in  
 1319 databases, support the creation of ontologies towards semantic information processing  
 1320 (MitoPedia), and help in communicating analytical findings as impactful data-driven  
 1321 stories. ‘*Making data available without making it understandable may be worse than not*  
 1322 *making it available at all*’ (National Academies of Sciences, Engineering, and Medicine  
 1323 2018). This is a call to carefully contribute to FAIR principles (Findable, Accessible,  
 1324 Interoperable, Reusable) for the sharing of scientific data.

1326 **Table 8. Terms, symbols, and units.**  
 1327  
 1328

1329 Term	Symbol	Unit	Links and comments
1330			
1331			
1332 alternative quinol oxidase	AOX		Fig. 2A
1333 amount of substance B	$n_B$	[mol]	
1334 cell number	$N_{\text{cell}}$	[x]	Tab. 5; $N_{\text{cell}} = N_{\text{vce}} + N_{\text{dce}}$
1335 cell viability index	$CVI$		$CVI = N_{\text{vce}}/N_{\text{cell}} = 1 - N_{\text{dce}}/N_{\text{cell}}$
1336 Complexes I to IV	CI to CIV		respiratory ET Complexes; Fig. 2A
1337 concentration of substance B	$c_B = n_B \cdot V^{-1}$ ; [B]	[mol·m <sup>-3</sup> ]	Box 2
1338 dead cell number	$N_{\text{dce}}$	[x]	Tab. 5; non-viable cells, loss of plasma membrane barrier function
1339			
1340 electron transfer system	ETS		Fig. 2A, Fig. 4
1341 flow, for substance B	$I_B$	[mol·s <sup>-1</sup> ]	system-related extensive quantity; Fig. 6
1342 flux, for substance B	$J_B$	<i>varies</i>	size-specific quantity; Fig. 6
1343 inorganic phosphate	$P_i$		Fig. 2C
1344 intact cell number, viable cell number	$N_{\text{vce}}$	[x]	Tab. 5; viable cells, intact of plasma membrane barrier function
1345			
1346 LEAK	LEAK		Tab. 1, Fig. 4
1347 mass of sample X	$m_X$	[kg]	Tab. 4
1348 mass of entity X	$M_X$	[kg]	mass of object X; Tab. 4
1349 MITOCARTA			<a href="https://www.broadinstitute.org/scientific-community/science/programs/metabolic-disease-program/publications/mitocarta/mitocarta-in-0">https://www.broadinstitute.org/scientific-community/science/programs/metabolic-disease-program/publications/mitocarta/mitocarta-in-0</a>
1350			
1351			
1352			
1353			
1354 MitoPedia			<a href="http://www.bioblast.at/index.php/MitoPedia">http://www.bioblast.at/index.php/MitoPedia</a>
1355 mitochondria or mitochondrial	mt		Box 1
1356 mitochondrial DNA	mtDNA		Box 1
1357 mitochondrial concentration	$C_{\text{mtE}} = \text{mtE} \cdot V^{-1}$	[mtEU·m <sup>-3</sup> ]	Tab. 4
1358 mitochondrial content	$\text{mtE}_X = \text{mtE} \cdot N_X^{-1}$	[mtEU·x <sup>-1</sup> ]	Tab. 4
1359 mitochondrial elemental unit	mtEU	<i>varies</i>	Tab. 4, specific units for mt-marker
1360 mitochondrial inner membrane	mtIM		Fig. 1; MIM is widely used; the first M is replaced by mt; Box 1
1361			
1362 mitochondrial outer membrane	mtOM		Fig. 1; MOM is widely used; the first M is replaced by mt; Box 1
1363			
1364 mitochondrial recovery	$Y_{\text{mtE}}$		fraction of <i>mtE</i> recovered in sample from the tissue of origin
1365			
1366 mitochondrial yield	$Y_{\text{mtE}/m}$		$Y_{\text{mtE}/m} = Y_{\text{mtE}} \cdot D_{\text{mtE}}$
1367 negative	neg		Fig. 2C
1368 number concentration of X	$C_{\text{NX}}$	[x·m <sup>-3</sup> ]	Tab. 4
1369 number of entities X	$N_X$	[x]	Tab. 4, Fig. 7
1370 number of entity B	$N_B$	[x]	Tab. 4

1371	oxidative phosphorylation	OXPHOS		Tab. 1, Fig. 4
1372	oxygen concentration	$c_{O_2} = n_{O_2} \cdot V^{-1}$ ; $[O_2]$	$[\text{mol} \cdot \text{m}^{-3}]$	Section 3.2
1373	permeabilized cell number	$N_{pce}$	$[x]$	Tab. 5; experimental permeabilization of plasma membrane; $N_{pce} = N_{cell}$
1374				
1375	phosphorylation of ADP to ATP	P»		Section 2.2
1376	positive	pos		Fig. 2C
1377	proton in the negative compartment	$H^{+}_{neg}$		Fig. 2C
1378	proton in the positive compartment	$H^{+}_{pos}$		Fig. 2C
1379	rate of electron transfer in ET state	$E$		ET-capacity; Tab. 1
1380	rate of LEAK respiration	$L$		Tab. 1
1381	rate of oxidative phosphorylation	$P$		OXPHOS capacity; Tab. 1
1382	rate of residual oxygen consumption	$Rox$		Tab. 1
1383	residual oxygen consumption	ROX		Tab. 1
1384	respiratory supercomplex	SC I <sub>n</sub> III <sub>n</sub> IV <sub>n</sub>		Box 1; supramolecular assemblies composed of variable copy numbers ( $n$ ) of CI, CIII and CIV
1385				
1386				
1387	specific mitochondrial density	$D_{mtE} = mtE \cdot m_X^{-1}$	$[\text{mtEU} \cdot \text{kg}^{-1}]$	Tab. 4
1388	volume	$V$	$[\text{m}^{-3}]$	Tab. 7
1389	weight, dry weight	$W_d$	$[\text{kg}]$	used as mass of sample X; Fig. 6
1390	weight, wet weight	$W_w$	$[\text{kg}]$	used as mass of sample X; Fig. 6
1391				

1392

1393

## 1394 Acknowledgements

1395 We thank M. Beno for management assistance. Supported by COST Action CA15203  
1396 MitoEAGLE and K-Regio project MitoFit (E.G.).

1397

1398 **Competing financial interests:** E.G. is founder and CEO of Oroboros Instruments, Innsbruck,  
1399 Austria.

1400

1401

## 1402 5. References

1403

1404 Altmann R (1894) Die Elementarorganismen und ihre Beziehungen zu den Zellen. Zweite vermehrte Auflage.  
1405 Verlag Von Veit & Comp, Leipzig:160 pp.

1406 Beard DA (2005) A biophysical model of the mitochondrial respiratory system and oxidative phosphorylation.  
1407 PLoS Comput Biol 1(4):e36.

1408 Benda C (1898) Weitere Mitteilungen über die Mitochondria. Verh Dtsch Physiol Ges:376-83.

1409 Birkedal R, Laasmaa M, Vendelin M (2014) The location of energetic compartments affects energetic  
1410 communication in cardiomyocytes. Front Physiol 5:376.

1411 Breton S, Beaupré HD, Stewart DT, Hoeh WR, Blier PU (2007) The unusual system of doubly uniparental  
1412 inheritance of mtDNA: isn't one enough? Trends Genet 23:465-74.

1413 Brown GC (1992) Control of respiration and ATP synthesis in mammalian mitochondria and cells. Biochem J  
1414 284:1-13.

1415 Calvo SE, Klauser CR, Mootha VK (2016) MitoCarta2.0: an updated inventory of mammalian mitochondrial  
1416 proteins. Nucleic Acids Research 44:D1251-7.

1417 Calvo SE, Julien O, Clauser KR, Shen H, Kamer KJ, Wells JA, Mootha VK (2017) Comparative analysis of  
1418 mitochondrial N-termini from mouse, human, and yeast. Mol Cell Proteomics 16:512-23.

1419 Campos JC, Queliconi BB, Bozi LHM, Bechara LRG, Dourado PMM, Andres AM, Jannig PR, Gomes KMS,  
1420 Zambelli VO, Rocha-Resende C, Guatimosim S, Brum PC, Mochly-Rosen D, Gottlieb RA, Kowaltowski AJ,  
1421 Ferreira JCB (2017) Exercise reestablishes autophagic flux and mitochondrial quality control in heart failure.  
1422 Autophagy 13:1304-317.

1423 Canton M, Luvisetto S, Schmehl I, Azzone GF (1995) The nature of mitochondrial respiration and  
1424 discrimination between membrane and pump properties. Biochem J 310:477-81.

1425 Chance B, Williams GR (1955a) Respiratory enzymes in oxidative phosphorylation. I. Kinetics of oxygen  
1426 utilization. J Biol Chem 217:383-93.

1427 Chance B, Williams GR (1955b) Respiratory enzymes in oxidative phosphorylation: III. The steady state. J Biol  
1428 Chem 217:409-27.

- 1429 Chance B, Williams GR (1955c) Respiratory enzymes in oxidative phosphorylation. IV. The respiratory chain. *J*  
 1430 *Biol Chem* 217:429-38.
- 1431 Chance B, Williams GR (1956) The respiratory chain and oxidative phosphorylation. *Adv Enzymol Relat Subj*  
 1432 *Biochem* 17:65-134.
- 1433 Cobb LJ, Lee C, Xiao J, Yen K, Wong RG, Nakamura HK, Mehta HH, Gao Q, Ashur C, Huffman DM, Wan J,  
 1434 Muzumdar R, Barzilai N, Cohen P (2016) Naturally occurring mitochondrial-derived peptides are age-  
 1435 dependent regulators of apoptosis, insulin sensitivity, and inflammatory markers. *Aging (Albany NY)* 8:796-  
 1436 809.
- 1437 Cohen ER, Cvitas T, Frey JG, Holmström B, Kuchitsu K, Marquardt R, Mills I, Pavese F, Quack M, Stohner J,  
 1438 Strauss HL, Takami M, Thor HL (2008) Quantities, units and symbols in physical chemistry, IUPAC Green  
 1439 Book, 3rd Edition, 2nd Printing, IUPAC & RSC Publishing, Cambridge.
- 1440 Cooper H, Hedges LV, Valentine JC, eds (2009) The handbook of research synthesis and meta-analysis. Russell  
 1441 Sage Foundation.
- 1442 Coopersmith J (2010) Energy, the subtle concept. The discovery of Feynman's blocks from Leibnitz to Einstein.  
 1443 Oxford University Press:400 pp.
- 1444 Cummins J (1998) Mitochondrial DNA in mammalian reproduction. *Rev Reprod* 3:172-82.
- 1445 Dai Q, Shah AA, Garde RV, Yonish BA, Zhang L, Medvitz NA, Miller SE, Hansen EL, Dunn CN, Price TM  
 1446 (2013) A truncated progesterone receptor (PR-M) localizes to the mitochondrion and controls cellular  
 1447 respiration. *Mol Endocrinol* 27:741-53.
- 1448 Divakaruni AS, Brand MD (2011) The regulation and physiology of mitochondrial proton leak. *Physiology*  
 1449 (Bethesda) 26:192-205.
- 1450 Doerrier C, Garcia-Souza LF, Krumschnabel G, Wohlfarter Y, Mészáros AT, Gnaiger E (2018) High-Resolution  
 1451 FluoRespirometry and OXPHOS protocols for human cells, permeabilized fibres from small biopsies of  
 1452 muscle and isolated mitochondria. *Methods Mol. Biol.* (in press)
- 1453 Doskey CM, van 't Erve TJ, Wagner BA, Buettner GR (2015) Moles of a substance per cell is a highly  
 1454 informative dosing metric in cell culture. *PLOS ONE* 10:e0132572.
- 1455 Drahota Z, Milerová M, Stieglerová A, Houstek J, Ostádal B (2004) Developmental changes of cytochrome *c*  
 1456 oxidase and citrate synthase in rat heart homogenate. *Physiol Res* 53:119-22.
- 1457 Duarte FV, Palmeira CM, Rolo AP (2014) The role of microRNAs in mitochondria: small players acting wide.  
 1458 *Genes (Basel)* 5:865-86.
- 1459 Ernster L, Schatz G (1981) Mitochondria: a historical review. *J Cell Biol* 91:227s-55s.
- 1460 Estabrook RW (1967) Mitochondrial respiratory control and the polarographic measurement of ADP:O ratios.  
 1461 *Methods Enzymol* 10:41-7.
- 1462 Faber C, Zhu ZJ, Castellino S, Wagner DS, Brown RH, Peterson RA, Gates L, Barton J, Bickett M, Hagerty L,  
 1463 Kimbrough C, Sola M, Bailey D, Jordan H, Elangbam CS (2014) Cardiolipin profiles as a potential  
 1464 biomarker of mitochondrial health in diet-induced obese mice subjected to exercise, diet-restriction and  
 1465 ephedrine treatment. *J Appl Toxicol* 34:1122-9.
- 1466 Fell D (1997) Understanding the control of metabolism. Portland Press.
- 1467 Garlid KD, Beavis AD, Ratkje SK (1989) On the nature of ion leaks in energy-transducing membranes. *Biochim*  
 1468 *Biophys Acta* 976:109-20.
- 1469 Garlid KD, Semrad C, Zinchenko V. Does redox slip contribute significantly to mitochondrial respiration? In:  
 1470 Schuster S, Rigoulet M, Ouhabi R, Mazat J-P, eds (1993) Modern trends in biothermokinetics. Plenum Press,  
 1471 New York, London:287-93.
- 1472 Gerö D, Szabo C (2016) Glucocorticoids suppress mitochondrial oxidant production via upregulation of  
 1473 uncoupling protein 2 in hyperglycemic endothelial cells. *PLoS One* 11:e0154813.
- 1474 Gnaiger E. Efficiency and power strategies under hypoxia. Is low efficiency at high glycolytic ATP production a  
 1475 paradox? In: *Surviving Hypoxia: Mechanisms of Control and Adaptation*. Hochachka PW, Lutz PL, Sick T,  
 1476 Rosenthal M, Van den Thillart G, eds (1993a) CRC Press, Boca Raton, Ann Arbor, London, Tokyo:77-109.
- 1477 Gnaiger E (1993b) Nonequilibrium thermodynamics of energy transformations. *Pure Appl Chem* 65:1983-2002.
- 1478 Gnaiger E (2001) Bioenergetics at low oxygen: dependence of respiration and phosphorylation on oxygen and  
 1479 adenosine diphosphate supply. *Respir Physiol* 128:277-97.
- 1480 Gnaiger E (2009) Capacity of oxidative phosphorylation in human skeletal muscle. New perspectives of  
 1481 mitochondrial physiology. *Int J Biochem Cell Biol* 41:1837-45.
- 1482 Gnaiger E (2014) Mitochondrial pathways and respiratory control. An introduction to OXPHOS analysis. 4th ed.  
 1483 *Mitochondr Physiol Network* 19.12. Oroboros MiPNet Publications, Innsbruck:80 pp.
- 1484 Gnaiger E, Méndez G, Hand SC (2000) High phosphorylation efficiency and depression of uncoupled respiration  
 1485 in mitochondria under hypoxia. *Proc Natl Acad Sci USA* 97:11080-5.
- 1486 Greggio C, Jha P, Kulkarni SS, Lagarrigue S, Broskey NT, Boutant M, Wang X, Conde Alonso S, Ofori E,  
 1487 Auwerx J, Cantó C, Amati F (2017) Enhanced respiratory chain supercomplex formation in response to  
 1488 exercise in human skeletal muscle. *Cell Metab* 25:301-11.
- 1489 Hinkle PC (2005) P/O ratios of mitochondrial oxidative phosphorylation. *Biochim Biophys Acta* 1706:1-11.



- 1490 Hofstadter DR (1979) Gödel, Escher, Bach: An eternal golden braid. A metaphorical fugue on minds and  
 1491 machines in the spirit of Lewis Carroll. Harvester Press:499 pp.
- 1492 Illaste A, Laasmaa M, Peterson P, Vendelin M (2012) Analysis of molecular movement reveals latticelike  
 1493 obstructions to diffusion in heart muscle cells. *Biophys J* 102:739-48.
- 1494 Jasienski M, Bazzaz FA (1999) The fallacy of ratios and the testability of models in biology. *Oikos* 84:321-26.
- 1495 Jepihhina N, Beraud N, Sepp M, Birkedal R, Vendelin M (2011) Permeabilized rat cardiomyocyte response  
 1496 demonstrates intracellular origin of diffusion obstacles. *Biophys J* 101:2112-21.
- 1497 Klepinin A, Ounpuu L, Guzun R, Chekulayev V, Timohhina N, Tepp K, Shevchuk I, Schlattner U, Kaambre T  
 1498 (2016) Simple oxygraphic analysis for the presence of adenylate kinase 1 and 2 in normal and tumor cells. *J*  
 1499 *Bioenerg Biomembr* 48:531-48.
- 1500 Klíngenberg M (2017) UCP1 - A sophisticated energy valve. *Biochimie* 134:19-27.
- 1501 Koit A, Shevchuk I, Ounpuu L, Klepinin A, Chekulayev V, Timohhina N, Tepp K, Puurand M, Truu L, Heck K,  
 1502 Valvere V, Guzun R, Kaambre T (2017) Mitochondrial respiration in human colorectal and breast cancer  
 1503 clinical material is regulated differently. *Oxid Med Cell Longev* 1372640.
- 1504 Komlódi T, Tretter L (2017) Methylene blue stimulates substrate-level phosphorylation catalysed by succinyl-  
 1505 CoA ligase in the citric acid cycle. *Neuropharmacology* 123:287-98.
- 1506 Lane N (2005) Power, sex, suicide: mitochondria and the meaning of life. Oxford University Press:354 pp.
- 1507 Larsen S, Nielsen J, Neigaard Nielsen C, Nielsen LB, Wibrand F, Stride N, Schroder HD, Boushel RC, Helge  
 1508 JW, Dela F, Hey-Mogensen M (2012) Biomarkers of mitochondrial content in skeletal muscle of healthy  
 1509 young human subjects. *J Physiol* 590:3349-60.
- 1510 Lee C, Zeng J, Drew BG, Sallam T, Martin-Montalvo A, Wan J, Kim SJ, Mehta H, Hevener AL, de Cabo R,  
 1511 Cohen P (2015) The mitochondrial-derived peptide MOTS-c promotes metabolic homeostasis and reduces  
 1512 obesity and insulin resistance. *Cell Metab* 21:443-54.
- 1513 Lee SR, Kim HK, Song IS, Youm J, Dizon LA, Jeong SH, Ko TH, Heo HJ, Ko KS, Rhee BD, Kim N, Han J  
 1514 (2013) Glucocorticoids and their receptors: insights into specific roles in mitochondria. *Prog Biophys Mol*  
 1515 *Biol* 112:44-54.
- 1516 Leek BT, Mudaliar SR, Henry R, Mathieu-Costello O, Richardson RS (2001) Effect of acute exercise on citrate  
 1517 synthase activity in untrained and trained human skeletal muscle. *Am J Physiol Regul Integr Comp Physiol*  
 1518 280:R441-7.
- 1519 Lemieux H, Blier PU, Gnaiger E (2017) Remodeling pathway control of mitochondrial respiratory capacity by  
 1520 temperature in mouse heart: electron flow through the Q-junction in permeabilized fibers. *Sci Rep* 7:2840.
- 1521 Lenaz G, Tioli G, Falasca AI, Genova ML (2017) Respiratory supercomplexes in mitochondria. In: Mechanisms  
 1522 of primary energy transduction in biology. M Wikstrom (ed) Royal Society of Chemistry Publishing, London,  
 1523 UK:296-337.
- 1524 Margulis L (1970) Origin of eukaryotic cells. New Haven: Yale University Press.
- 1525 Meinild Lundby AK, Jacobs RA, Gehrig S, de Leur J, Hauser M, Bonne TC, Flück D, Dandanell S, Kirk N,  
 1526 Kaech A, Ziegler U, Larsen S, Lundby C (2018) Exercise training increases skeletal muscle mitochondrial  
 1527 volume density by enlargement of existing mitochondria and not de novo biogenesis. *Acta Physiol* 222,  
 1528 e12905.
- 1529 Menshikova EV, Ritov VB, Fairfull L, Ferrell RE, Kelley DE, Goodpaster BH (2006) Effects of exercise on  
 1530 mitochondrial content and function in aging human skeletal muscle. *J Gerontol A Biol Sci Med Sci* 61:534-  
 1531 40.
- 1532 Menshikova EV, Ritov VB, Ferrell RE, Azuma K, Goodpaster BH, Kelley DE (2007) Characteristics of skeletal  
 1533 muscle mitochondrial biogenesis induced by moderate-intensity exercise and weight loss in obesity. *J Appl*  
 1534 *Physiol* (1985) 103:21-7.
- 1535 Menshikova EV, Ritov VB, Toledo FG, Ferrell RE, Goodpaster BH, Kelley DE (2005) Effects of weight loss  
 1536 and physical activity on skeletal muscle mitochondrial function in obesity. *Am J Physiol Endocrinol Metab*  
 1537 288:E818-25.
- 1538 Miller GA (1991) The science of words. Scientific American Library New York:276 pp.
- 1539 Mitchell P (1961) Coupling of phosphorylation to electron and hydrogen transfer by a chemi-osmotic type of  
 1540 mechanism. *Nature* 191:144-8.
- 1541 Mitchell P (2011) Chemiosmotic coupling in oxidative and photosynthetic phosphorylation. *Biochim Biophys*  
 1542 *Acta Bioenergetics* 1807:1507-38.
- 1543 Mogensen M, Sahlin K, Fernström M, Glinthorg D, Vind BF, Beck-Nielsen H, Højlund K (2007) Mitochondrial  
 1544 respiration is decreased in skeletal muscle of patients with type 2 diabetes. *Diabetes* 56:1592-9.
- 1545 Mohr PJ, Phillips WD (2015) Dimensionless units in the SI. *Metrologia* 52:40-7.
- 1546 Moreno M, Giacco A, Di Munno C, Goglia F (2017) Direct and rapid effects of 3,5-diiodo-L-thyronine (T2).  
 1547 *Mol Cell Endocrinol* 7207:30092-8.
- 1548 Morrow RM, Picard M, Derbeneva O, Leipzig J, McManus MJ, Gouspillou G, Barbat-Artigas S, Dos Santos C,  
 1549 Hepple RT, Murdock DG, Wallace DC (2017) Mitochondrial energy deficiency leads to hyperproliferation of  
 1550 skeletal muscle mitochondria and enhanced insulin sensitivity. *Proc Natl Acad Sci U S A* 114:2705-10.
- 1551 Murley A, Nunnari J (2016) The emerging network of mitochondria-organelle contacts. *Mol Cell* 61:648-53.

- 1552 National Academies of Sciences, Engineering, and Medicine (2018) International coordination for science data  
 1553 infrastructure: Proceedings of a workshop—in brief. Washington, DC: The National Academies Press. doi:  
 1554 <https://doi.org/10.17226/25015>.
- 1555 Paradies G, Paradies V, De Benedictis V, Ruggiero FM, Petrosillo G (2014) Functional role of cardiolipin in  
 1556 mitochondrial bioenergetics. *Biochim Biophys Acta* 1837:408-17.
- 1557 Pesta D, Gnaiger E (2012) High-Resolution Respirometry. OXPHOS protocols for human cells and  
 1558 permeabilized fibres from small biopsies of human muscle. *Methods Mol Biol* 810:25-58.
- 1559 Pesta D, Hoppel F, Macek C, Messner H, Faulhaber M, Kobel C, Parson W, Burtscher M, Schocke M, Gnaiger  
 1560 E (2011) Similar qualitative and quantitative changes of mitochondrial respiration following strength and  
 1561 endurance training in normoxia and hypoxia in sedentary humans. *Am J Physiol Regul Integr Comp Physiol*  
 1562 301:R1078–87.
- 1563 Price TM, Dai Q (2015) The role of a mitochondrial progesterone receptor (PR-M) in progesterone action.  
 1564 *Semin Reprod Med* 33:185-94.
- 1565 Puchowicz MA, Varnes ME, Cohen BH, Friedman NR, Kerr DS, Hoppel CL (2004) Oxidative phosphorylation  
 1566 analysis: assessing the integrated functional activity of human skeletal muscle mitochondria – case studies.  
 1567 *Mitochondrion* 4:377-85. Puntschart A, Claassen H, Jostardt K, Hoppeler H, Billeter R (1995) mRNAs of  
 1568 enzymes involved in energy metabolism and mtDNA are increased in endurance-trained athletes. *Am J*  
 1569 *Physiol* 269:C619-25.
- 1570 Quiros PM, Mottis A, Auwerx J (2016) Mitonuclear communication in homeostasis and stress. *Nat Rev Mol*  
 1571 *Cell Biol* 17:213-26.
- 1572 Rackham O, Mercer TR, Filipovska A (2012) The human mitochondrial transcriptome and the RNA-binding  
 1573 proteins that regulate its expression. *WIREs RNA* 3:675–95.
- 1574 Reichmann H, Hoppeler H, Mathieu-Costello O, von Bergen F, Pette D (1985) Biochemical and ultrastructural  
 1575 changes of skeletal muscle mitochondria after chronic electrical stimulation in rabbits. *Pflugers Arch* 404:1-  
 1576 9.
- 1577 Renner K, Amberger A, Konwalinka G, Gnaiger E (2003) Changes of mitochondrial respiration, mitochondrial  
 1578 content and cell size after induction of apoptosis in leukemia cells. *Biochim Biophys Acta* 1642:115-23.
- 1579 Rich P (2003) Chemiosmotic coupling: The cost of living. *Nature* 421:583.
- 1580 Rostovtseva TK, Sheldon KL, Hassanzadeh E, Monge C, Saks V, Bezrukov SM, Sackett DL (2008) Tubulin  
 1581 binding blocks mitochondrial voltage-dependent anion channel and regulates respiration. *Proc Natl Acad Sci*  
 1582 *USA* 105:18746-51.
- 1583 Rustin P, Parfait B, Chretien D, Bourgeron T, Djouadi F, Bastin J, Rötig A, Munnich A (1996) Fluxes of  
 1584 nicotinamide adenine dinucleotides through mitochondrial membranes in human cultured cells. *J Biol Chem*  
 1585 271:14785-90.
- 1586 Saks VA, Veksler VI, Kuznetsov AV, Kay L, Sikk P, Tiivel T, Tranqui L, Olivares J, Winkler K, Wiedemann F,  
 1587 Kunz WS (1998) Permeabilised cell and skinned fiber techniques in studies of mitochondrial function in  
 1588 vivo. *Mol Cell Biochem* 184:81-100.
- 1589 Salabei JK, Gibb AA, Hill BG (2014) Comprehensive measurement of respiratory activity in permeabilized cells  
 1590 using extracellular flux analysis. *Nat Protoc* 9:421-38.
- 1591 Sazanov LA (2015) A giant molecular proton pump: structure and mechanism of respiratory complex I. *Nat Rev*  
 1592 *Mol Cell Biol* 16:375-88.
- 1593 Schneider TD (2006) Claude Shannon: biologist. The founder of information theory used biology to formulate  
 1594 the channel capacity. *IEEE Eng Med Biol Mag* 25:30-3.
- 1595 Schönfeld P, Dymkowska D, Wojtczak L (2009) Acyl-CoA-induced generation of reactive oxygen species in  
 1596 mitochondrial preparations is due to the presence of peroxisomes. *Free Radic Biol Med* 47:503-9.
- 1597 Schultz J, Wiesner RJ (2000) Proliferation of mitochondria in chronically stimulated rabbit skeletal muscle--  
 1598 transcription of mitochondrial genes and copy number of mitochondrial DNA. *J Bioenerg Biomembr* 32:627-  
 1599 34.
- 1600 Spejjer D (2016) Being right on Q: shaping eukaryotic evolution. *Biochem J* 473:4103-27.
- 1601 Sugiura A, Mattie S, Prudent J, McBride HM (2017) Newly born peroxisomes are a hybrid of mitochondrial and  
 1602 ER-derived pre-peroxisomes. *Nature* 542:251-4.
- 1603 Simson P, Jephthina N, Laasmaa M, Peterson P, Birkedal R, Vendelin M (2016) Restricted ADP movement in  
 1604 cardiomyocytes: Cytosolic diffusion obstacles are complemented with a small number of open mitochondrial  
 1605 voltage-dependent anion channels. *J Mol Cell Cardiol* 97:197-203.
- 1606 Stucki JW, Ineichen EA (1974) Energy dissipation by calcium recycling and the efficiency of calcium transport  
 1607 in rat-liver mitochondria. *Eur J Biochem* 48:365-75.
- 1608 Tonkonogi M, Harris B, Sahlin K (1997) Increased activity of citrate synthase in human skeletal muscle after a  
 1609 single bout of prolonged exercise. *Acta Physiol Scand* 161:435-6.
- 1610 Vamecq J, Schepers L, Parmentier G, Mannaerts GP (1987) Inhibition of peroxisomal fatty acyl-CoA oxidase by  
 1611 antimycin A. *Biochem J* 248:603-7.

- 1612 Waczulikova I, Habodaszova D, Cagalinec M, Ferko M, Ulicna O, Mateasik A, Sikurova L, Ziegelhöffer A  
1613 (2007) Mitochondrial membrane fluidity, potential, and calcium transients in the myocardium from acute  
1614 diabetic rats. *Can J Physiol Pharmacol* 85:372-81.
- 1615 Wagner BA, Venkataraman S, Buettner GR (2011) The rate of oxygen utilization by cells. *Free Radic Biol Med*  
1616 51:700-712.
- 1617 Wang H, Hiatt WR, Barstow TJ, Brass EP (1999) Relationships between muscle mitochondrial DNA content,  
1618 mitochondrial enzyme activity and oxidative capacity in man: alterations with disease. *Eur J Appl Physiol*  
1619 *Occup Physiol* 80:22-7.
- 1620 Watt IN, Montgomery MG, Runswick MJ, Leslie AG, Walker JE (2010) Bioenergetic cost of making an  
1621 adenosine triphosphate molecule in animal mitochondria. *Proc Natl Acad Sci U S A* 107:16823-7.
- 1622 Weibel ER, Hoppeler H (2005) Exercise-induced maximal metabolic rate scales with muscle aerobic capacity. *J*  
1623 *Exp Biol* 208:1635-44.
- 1624 White DJ, Wolff JN, Pierson M, Gemmell NJ (2008) Revealing the hidden complexities of mtDNA inheritance.  
1625 *Mol Ecol* 17:4925-42.
- 1626 Wikström M, Hummer G (2012) Stoichiometry of proton translocation by respiratory complex I and its  
1627 mechanistic implications. *Proc Natl Acad Sci U S A* 109:4431-6.
- 1628 Willis WT, Jackman MR, Messer JI, Kuzmiak-Glancy S, Glancy B (2016) A simple hydraulic analog model of  
1629 oxidative phosphorylation. *Med Sci Sports Exerc* 48:990-1000.